U.S.N.A---Trident Scholar project report; no xxx (2002)

BIOPHYSICAL CHARACTERIZATION OF A BIFUNCTIONAL IRON REGULATING ENZYME

By

Midshipman Pritha M. Mahadevan, Class of 2002
United States Naval Academy
Annapolis, Maryland

(signature)

Certification of Adviser Approval

Assistant Professor Virginia F. Smith
Department of Chemistry

(signature)

(date)

Acceptance for the Trident Scholar Committee

Professor Joyce E. Shade
Deputy Director of Research

(signature)

(date)

USNA-1531-2

REPORT DOCUMENTATION PAGE	Form Approved OMB No. 0704-0188

1. REPORT DATE (DD-MM-YYYY) 07-05-2002	2. REPORT TYPE	3. DATES COVERED (FROM - TO) xx-xx-2002 to xx-xx-2002

4. TITLE AND SUBTITLE Bifunctional Characterization of an Iron Regulating Enzyme Unclassified	5a. CONTRACT NUMBER 5b. GRANT NUMBER 5c. PROGRAM ELEMENT NUMBER
6. AUTHOR(S) Mahadevan, Pritha M. ;	5d. PROJECT NUMBER 5e. TASK NUMBER 5f. WORK UNIT NUMBER
7. PERFORMING ORGANIZATION NAME AND ADDRESS US Naval Academy Annapolis, MD21402	8. PERFORMING ORGANIZATION REPORT NUMBER
9. SPONSORING/MONITORING AGENCY NAME AND ADDRESS ,	10. SPONSOR/MONITOR'S ACRONYM(S) 11. SPONSOR/MONITOR'S REPORT NUMBER(S)

12. DISTRIBUTION/AVAILABILITY STATEMENT
APUBLIC RELEASE
,

13. SUPPLEMENTARY NOTES

14. ABSTRACT
See report.

15. SUBJECT TERMS

16. SECURITY CLASSIFICATION OF:			17. LIMITATION OF ABSTRACT	18. NUMBER OF PAGES	19. NAME OF RESPONSIBLE PERSON
			Public Release	69	email from USNA, (blank) lfenster@dtic.mil
a. REPORT Unclassified	b. ABSTRACT Unclassified	c. THIS PAGE Unclassified			19b. TELEPHONE NUMBER International Area Code Area Code Telephone Number 703767-9007 DSN 427-9007

REPORT DOCUMENTATION PAGE

Form Approved
OMB No. 074-0188

1. AGENCY USE ONLY (Leave blank)	2. REPORT DATE	3. REPORT TYPE AND DATE COVERED
	7 May 2002	

4. TITLE AND SUBTITLE
Biophysical characterization of a bifunctional iron regulating enzyme

5. FUNDING NUMBERS

6. AUTHOR(S)
Mahadevan, Pritha M. (Pritha Mathangi), 1979-

7. PERFORMING ORGANIZATION NAME(S) AND ADDRESS(ES)

8. PERFORMING ORGANIZATION REPORT NUMBER

9. SPONSORING/MONITORING AGENCY NAME(S) AND ADDRESS(ES)
US Naval Academy
Annapolis, MD 21402

10. SPONSORING/MONITORING AGENCY REPORT NUMBER
Trident Scholar project report no. 298 (2002)

11. SUPPLEMENTARY NOTES

12a. DISTRIBUTION/AVAILABILITY STATEMENT
This document has been approved for public release; its distribution is UNLIMITED.

12b. DISTRIBUTION CODE

13. ABSTRACT: n recent years, proteins have been discovered that can interchange forms and conduct two distinct functions. One such polypeptide with two specific functions is the mammalian iron responsive element (IRE) binding protein IRP-1. When iron levels within the cell are normal, this protein contains an iron-sulfur cluster and is known as cytoplasmic aconitase, an enzyme that catalyzes a specific chemical reaction. When iron levels fall below normal, however, the iron-sulfur cluster is lost, the protein loses its enzymatic activity and it becomes IRP-1, which binds to certain regions of ribonucleic acid (RNA). This binding action helps restore iron levels to normal, and in the process returns the protein to its cytoplasmic aconitase form. In order to understand the structural features that stabilize this large bifunctional protein, folding studies were performed in the presence and absence of iron on a recombinant version of the human protein. Equilibrium unfolding experiments in urea revealed that huma n cytoplasmic aconitase undergoes a multi-state transition from the native to denatured form. Comparison of unfolding in the presence and absence of the [4Fe-4S] cluster indicate that the cluster does not have a significant effect on the equilibrium unfolding properties as monitored by fluorescence. Monitoring enzymatic activity as a function of urea concentration indicates that activity is lost at ~2M urea, presumably due to disruption of the enzyme active site, which is at the major interdomain cleft. The effect of thermal denaturation on the stability and activity of the IRP-1 was also studied. A preliminary model for the unfolding of aconitase based on its enzyme activity, equilibrium thermal properties, and chemical denaturation data is presented.

14. SUBJECT TERMS
cytoplasmic aconitase, IRP-1, protein folding, fluorescence spectroscopy, iron regulation

15. NUMBER OF PAGES
69

16. PRICE CODE

17. SECURITY CLASSIFICATION OF REPORT	18. SECURITY CLASSIFICATION OF THIS PAGE	19. SECURITY CLASSIFICATION OF ABSTRACT	20. LIMITATION OF ABSTRACT

ABSTRACT

In recent years, proteins have been discovered that can interchange forms and conduct two distinct functions. One such polypeptide with two specific functions is the mammalian iron responsive element (IRE) binding protein IRP-1. When iron levels within the cell are normal, this protein contains an iron-sulfur cluster and is known as cytoplasmic aconitase, an enzyme that catalyzes a specific chemical reaction. When iron levels fall below normal, however, the iron-sulfur cluster is lost, the protein loses its enzymatic activity and it becomes IRP-1, which binds to certain regions of ribonucleic acid (RNA). This binding action helps restore iron levels to normal, and in the process returns the protein to its cytoplasmic aconitase form.

In order to understand the structural features that stabilize this large bifunctional protein, folding studies were performed in the presence and absence of iron on a recombinant version of the human protein. Equilibrium unfolding experiments in urea revealed that human cytoplasmic aconitase undergoes a multi-state transition from the native to denatured form. Comparison of unfolding in the presence and absence of the [4Fe-4S] cluster indicate that the cluster does not have a significant effect on the equilibrium unfolding properties as monitored by fluorescence. Monitoring enzymatic activity as a function of urea concentration indicates that activity is lost at ~2M urea, presumably due to disruption of the enzyme active site, which is at the major interdomain cleft. The effect of thermal denaturation on the stability and activity of the IRP-1 was also studied. A preliminary model for the unfolding of aconitase based on its enzyme activity, equilibrium thermal properties, and chemical denaturation data is presented.

Keywords: cytoplasmic aconitase, IRP-1, protein folding, fluorescence spectroscopy, iron regulation

Acknowledgements

During the course of this research project, countless individuals have taken extensive amounts of time to instruct, teach, and guide me through the difficulties and rewards of research. I would like to take time to thank the following people in particular:

Clarene Mullin, for always helping me with biological laboratory equipment and for having the patience to always re-teach me

Professor Judith Hartman, for aiding in the EPR experiments

Professor Robert Ferrante, for helping me understand the principles behind fluorescence spectroscopy.

Professor Fowler and Professor Turner, for agreeing to teach the Trident "cohort" about data analysis and statistics. I thoroughly enjoyed the class.

Mrs. Lynne Fenwick, for graciously handling all the travel arrangements and travel claims

I would like to especially thank Dean Miller, Academic Dean, US Naval Academy, and the Trident Committee for allowing me to spend my senior year devoted to research. The financial and institutional support has been phenomenal, and I am indebted for this exceptional experience.

Finally, I cannot begin to express my gratitude to Dr. Virginia Smith, my advisor. Throughout the project, she always had infinite patience to teach me, guide me, correct me, and often help me keep life and research in the proper perspective. Without a doubt, the entire success of this project is a result of her professional dedication and commitment to me, the Naval Academy, and the pursuit of scientific knowledge. Thank you.

Table of Contents

I. Background

Proteins are the most diverse class of biological macromolecules, seen in every form of life. Proteins, the most common expression of genetic information, vary greatly with respect to their size. All proteins are extraordinarily complex and varied, and all proteins are composed of the same class of monomeric unit, the amino acid. From a common set of 20 amino acids, biological products such as enzymes, hormones, antibodies, and muscle are produced. Of these types of proteins, the enzyme is the most specialized, catalyzing virtually all cellular reactions (Nelson & Cox).

The structure of a protein is critical to its function because the action of an enzyme depends on a specific interaction between an active site of the protein and the chemical substrate.

Protein structure is usually described in four levels. The first level describes the basic linear sequence of the amino acid synthesis. The second level refers to local interactions between amino acids (Nelson & Cox), with the two most common arrangements being beta sheets and alpha helices.

The third structural level is the most critical level for the action of enzymes. The tertiary structure describes the three dimensional arrangement of amino acid residues which result from specific placement of secondary structure elements. The tertiary structures of proteins are held together primarily by hydrophobic interactions, electrostatic charges, and hydrogen bonding.

The fourth structural level, which is not relevant to the protein being studied in this project, describes multi-unit proteins and their spatial orientation.

For an enzyme to function properly, it must be in its native state, which is the most stable, thermodynamically favored form. A protein can be denatured, or unfolded, from its native

conformation by changes in intracellular conditions such as pH, salinity, and temperature. Once a protein is denatured, it loses its stability, and therefore its function.

One approach to solving the "protein-folding problem" in biochemistry is to determine the stability of a protein, by carefully controlled denaturation. In order to fully understand the specific purpose and mechanism of a given protein, the structure and stability must be determined experimentally.

For many years, the biochemical dogma was that each synthesized protein possessed one specific function, and that the protein would not be able to change forms into another functional protein. More recently, however, proteins have been discovered that can interchange forms and perform two distinct functions. Specifically, a new class of proteins is emerging, and these proteins are enzymes with seemingly unrelated secondary functions as nucleic acid binding proteins (Paraskeva et al, 1996).

An example of a single polypeptide with two specific functions is the mammalian iron responsive element (IRE) binding protein IRP-1. The human iron responsive protein (h-IRP) is a 98 kDa, monomeric, four-domain protein consisting of 889 amino acid residues. The IRE, or iron responsive element, is a segment of RNA (ribonucleic acid) that influences iron uptake. During times of low iron levels, the IRP-1 binds to the IRE and produces more proteins involved in iron metabolism, resulting in restoration of proper iron levels. Once iron levels are high enough, the IRP-1 loses its affinity for the IRE.

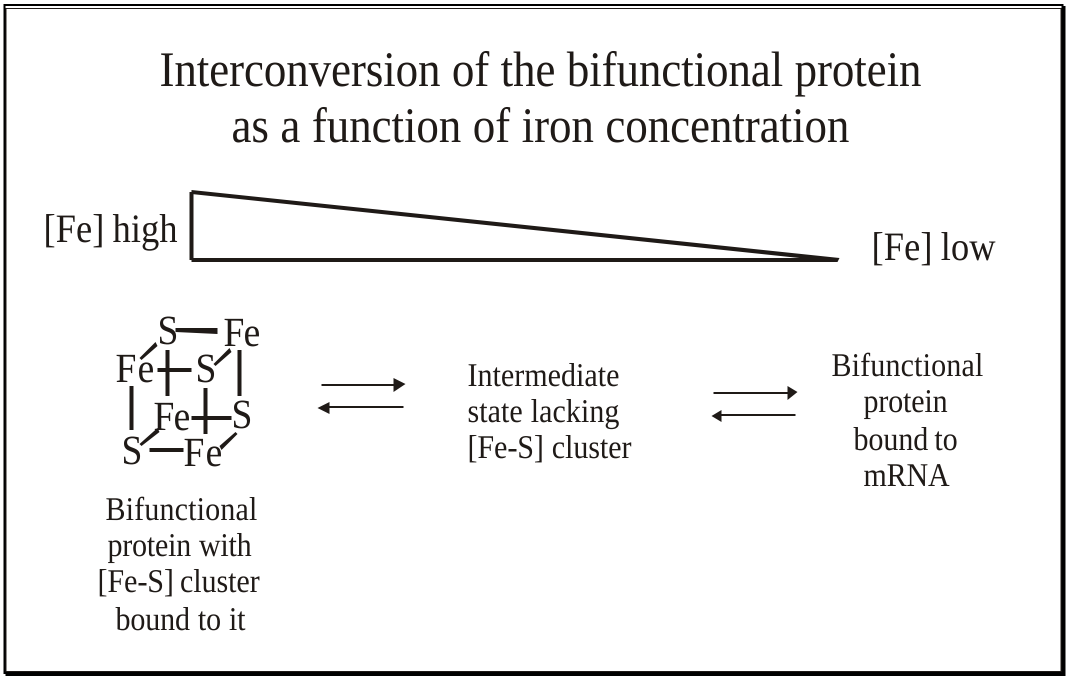

Figure 1 The above figure illustrates the iron-regulating mechanism of h-IRP1 and cytoplasmic aconitase (Smith, 2001)

The conversion of the IRP-1 to the enzyme aconitase is the unique feature of this protein. When iron levels become sufficiently high in the cell, an iron-sulfur cluster is assembled within the protein, possibly, as a means to properly sense and regulate the excess iron. With the addition of the iron-sulfur cluster, the IRP-1 assumes its other form of cytoplasmic aconitase. The cytoplasmic aconitase has the same enzymatic activity as mitochondrial aconitase. Mitochondrial aconitase performs a critical function in the central metabolic process, the Krebs cycle, by converting citrate to isocitrate. The cytoplasmic aconitase, however, is retained within the cytoplasm and does not participate in the Kreb's cycle. Iron levels within the mammal control the inter-converting mechanism.

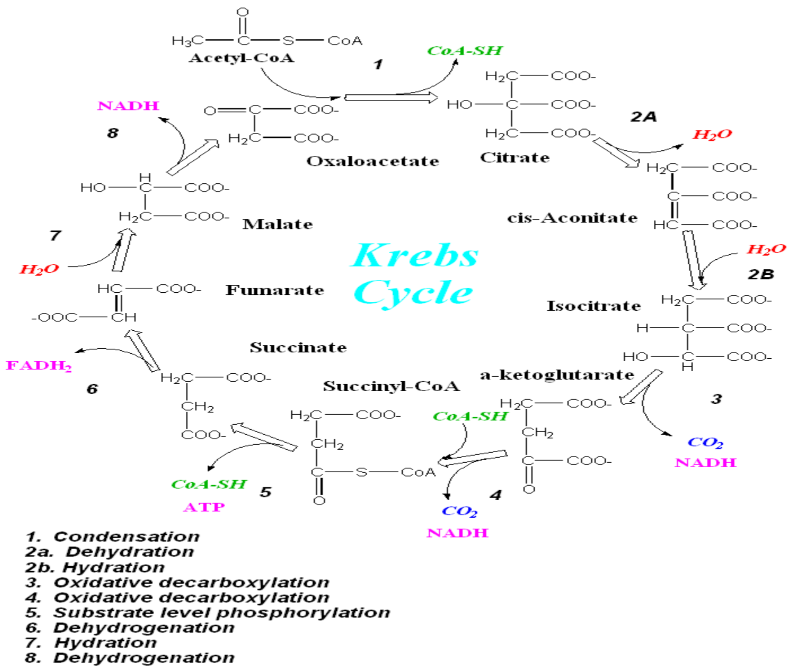

Figure 2 The above diagram shows the Kreb's cycle found in the mitochondria of all human cells.
http://wine1.sb.fsu.edu/krebs/krebs.htm

The structure of porcine mitochondrial aconitase has been well studied and documented by means of high resolution X-ray crystallography; however, there is currently no detailed information regarding either the structure or equilibrium properties of cytoplasmic aconitase and IRP-1. Thus, extensive characterization must be performed in order to better understand the mechanisms of this protein.

Objectives of Characterization Efforts

In this characterization study, the purpose was to observe denaturation of cytoplasmic aconitase through spectroscopic and enzymatic methods. An increased understanding of the stabilizing effects of the iron-sulfur cluster was sought, as was gaining insight to structural features distinguishing the large, multi-domained protein.

This project also investigated the mechanism of aconitase unfolding to seek a possible correlation between cluster activity and unfolded state. Finally, a quantitative value was sought by means of thermal denaturation to gain a better sense of the protein's overall stability at its folded, native state.

The study of the characteristics of the iron-sulfur protein aconitase will give insight into the regulation of iron, a scarce but vital mineral, at the cellular level. This project also provides a greater understanding of the nature of rare, bifunctional proteins. The challenges of modern biology include correlating a protein structure to a definite three-dimensional structure and the subsequent function.

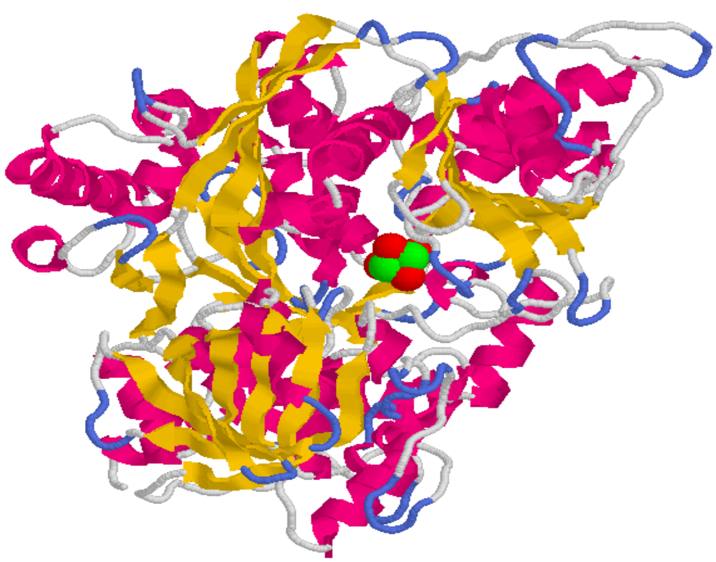

Figure 3 This three dimensional representation of the porcine *m*-aconitase shows the protein scaffolding and the iron-sulfur center as the red/green center
http://chemistry.gsu.edu/glactone/PDB/Proteins/Krebs/6acn.html

II. Experimental Methods

Synthesis and Purification of IRP-1/c-aconitase

Before the folding properties could be investigated, it was necessary to obtain pure enzyme. Although the enzyme being studied was the human form of the protein, it was produced in bacteria using recombinant methods.

When attempting to characterize any biological product, a method for obtaining a substantial sample must be developed. In studying human IRP, lysing actual human cells and then attempting to purify h-IRP would be unrealistic and impractical. A sample of lysed human cells would contain so many other cellular products that purification would be extremely difficult.

Therefore, the technique employed utilizes recombinant genetic technology. In recombinant methods, a segment of DNA is spliced from the original source and then inserted into a host for the explicit purpose of mass overexpression. The principal genetic tool used is a plasmid, a short, circular DNA fragment that once altered, is easily absorbed by bacteria. The altered plasmid becomes a part of the bacteria's genes, and as the bacteria undergoes metabolic processes, the desired genetic product is also produced. It should be noted that the high rate of protein production results from bacteria genomes absorbing up to thousands of plasmids; as the cell divides, plasmid proliferation continues, increasing IRP synthesis.

Simply put, DNA from the desired gene is cut by enzymes that recognize specific gene sequences and is then inserted into a host gene. The host gene is then absorbed into the genetic sequence of a host organism, most likely a bacteria, and the bacteria will produce the desired genetic product in large quantities.

Along with inserting the actual genetic material, a marker gene is also inserted to serve as a control mechanism. The marker gene normally confers some advantageous characteristic to the transformed bacteria. Resistance to an antibiotic is the most commonly used control. The resistance gene provides two functions, both beneficial to the multiplying host bacteria cell. First, the gene serves as a control marker. If the transformed plasmid is properly inserted into the genetic sequence of the host bacteria, and the host bacteria is grown in a nutrient broth containing an antibiotic, only the transformed bacteria will survive due to the resistance conferred by the inserted gene.

Second, the addition of the plasmid into the bacterial genome produces an enormous amount of stress on the metabolic capabilities of the bacteria. Without the stress of an antibiotic, the bacteria would reject the plasmid and with it the desired gene sequence needing expression. The added resistance gained provides enough incentive for the bacteria to retain the plasmid and incur the retention stress when in an environment containing an antibiotic.

The gene for the h-IRP1 protein is encoded within a plasmid in *E.coli*. The *E.coli* has been transformed with a plasmid containing the hIRP-1 sequence and a marker plasmid called AMP^r. The marker strain is used to verify if the plasmid was successfully incorporated into the bacteria. Based on experimental controls, the successfully modified bacteria will produce β-lactamase. β-lactamase is an enzyme that allows the bacteria to resist the anti-bacterial effects of ampicillin.

The plasmid, containing hIRP-1 and AMP^r was provided by Matthias Hentze, European Molecular Biology Laboratories, Heidelberg, Germany. The bacterial strain (BL-21 DE3) was a gift from the laboratory of C. Robert Matthews at University of Massachusetts Medical School, Worcester, Massachuasetts. The bacterial strain and plasmid are stored in a –70°C freezer.

Bacteria Plating and Cultures

The bacterial strain transformed with the plasmid was streaked onto agar plates and incubated overnight at 37ºC. The agar plates were prepared with and without the antibiotic ampicillin. The ampicillin (50 μg/mL) in the agar medium is used to kill any bacteria not transformed with the ampicillin resistant marker. The following table and pictures clearly show the control and experimental growths. The notation Ap(50) indicates an ampicillin concentration of 50 μg/mL in the agar solution.

Growth Plate Media Composition	Expected Results (all expected results were met as evidenced in the below pictures)
hIRP-1/BL 21 (DE3) on LB-Ap(50)	Growth observed, less than untransformed bacteria
hIRP1/BL 21 (DE3) on LB	More growth observed due to lack of environmental stress
BL 21 (DE3) on LB	Normal growth observed
BL 21 (DE3) on LB-Ap(50)	No growth observed due to antibiotic

Figure 4 The Ap(50) indicates plate with antibacterial ampicillin, hIRP-1/ BL 21 (DE3) is the transformed bacteria, and LB is the general broth media used to provide nutrition to the growing bacteria.

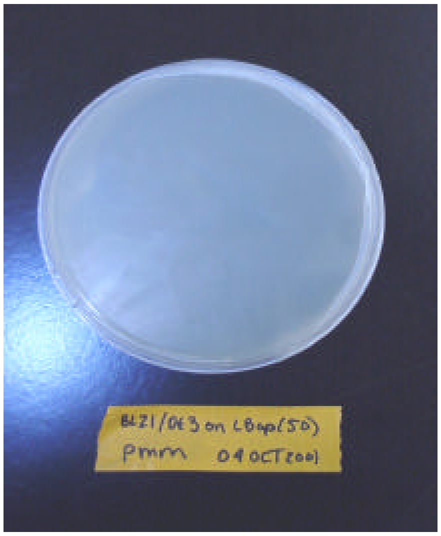

Figure 5 The *E.coli* bacteria did not grow untransformed due to the presence of ampicillin.

Figure 6 The transformed *E. coli* bacteria has grown in greater quantities in the absence of antibiotic. Without an environmental stress, the bacteria has little incentive to expend valuable cellular energy in keeping the plasmid. The extra energy can be spent on reproduction as seen in the plate.

Figure 7 In contrast to the above plate, the transformed *E.coli* in the presence of antibiotic must expend energy to survive and therefore produces fewer colonies than in the absence of ampicillin.

Figure 8 The untransformed *E .coli* grows on LB agar media as expected.

Small Scale Culture

After the transformed bacteria were plated out, and the transformation was verified, a small scale culture was grown. Using 1 mL of sterile LB broth solution, 5 µL of 10mg/mL ampicillin, and a scrape of bacteria from the one experimental plate, the small-scale culture was grown overnight in a New Brunswick shaking incubator at 25°C and 150 rpm (revolutions per minute).

When selecting bacteria for the culture, single, isolated colonies were chosen because this indicated no untransformed *E. coli* was present. As stated earlier, transformed bacteria secrete β-lactamase, and the secreted enzyme confers resistance to surrounding colonies, which may not be transformed. Therefore it is important to select isolated, single colonies because this assures that it contains the plasmid and did not get resistance from a nearby colony.

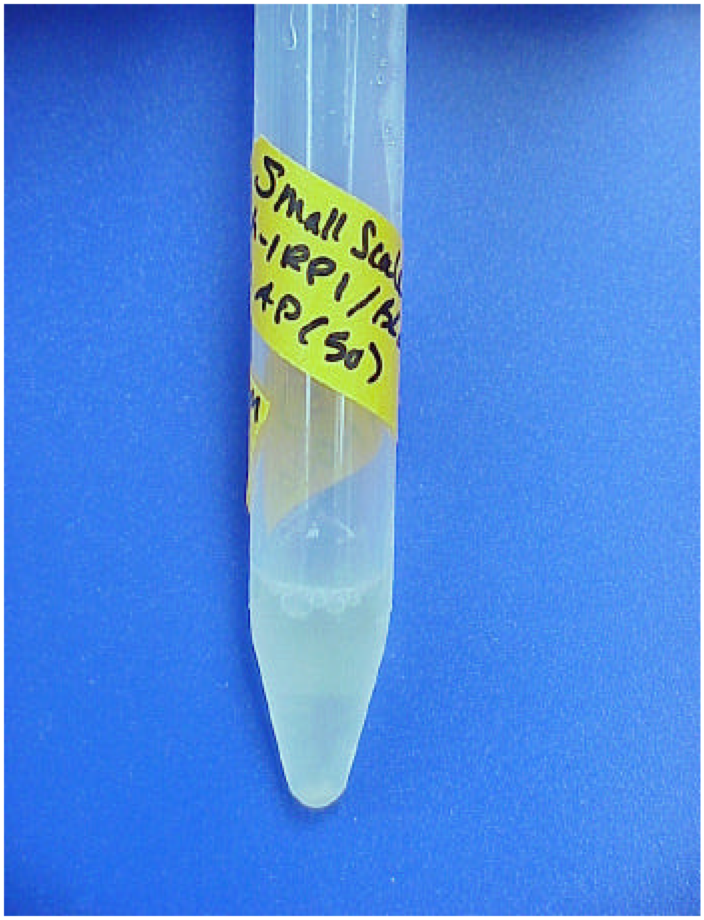

Figure 9 The small-scale culture yields a cloudy solution in an otherwise sterile LB-broth.

Large Scale Culture

After insuring normal growth of the small scale culture, a large scale culture is grown to produce the actual protein on which later characterization experiments will be conducted.

Two 2.8 L Fernbach flasks, large, flat-bottomed flasks which provide good aeration, are used, and 20 g of Sigma Chemical Company LB broth are dissolved into 1 liter of tap water. The tap water is used to give the *E. coli* bacteria an opportunity to find mineral species from which to construct the aconitase's iron-sulfur center.

The threat of bacterial contamination is always present, and two precautions are taken to produce the most sterile media possible for the bacteria. First, 50 mg of ampicillin are added to the large-scale culture to kill any foreign bacteria, and since the *E.coli* has been transformed with an ampicillin resistant strain, the aconitase-producing bacteria will not be destroyed by the antibiotic.

The second precaution taken consists of using an autoclave to sterilize the LB broth before ampicillin and bacterial culture are added. The autoclave is an instrument that raises the pressure to 15 psi and temperature to 121°C, and these conditions sufficiently kill bacteria. The high pressure of the autoclave prevents evaporation of the solution. After twenty minutes of intense temperatures, the dissolved LB broth is considered sterile.

After cooling the autoclaved broth to less than 50°C, 5 mL of a 10 mg/mL ampicillin solution and 1 mL of the small scale culture are added. The two 1 L inoculated flasks are incubated overnight at a temperature of 25°C and at 175 rpm. The constant motion provided by the 175 rpm prevents an overgrowth on the solution surface that would cause bacteria to not grow from lack of oxygen.

Cell Lysing and Protein Harvesting

After being grown overnight, the bacterial cells are ready to be harvested and lysed. The bacterial broth is poured into four plastic jars that fit into a swinging bucket centrifuge rotor. The four jars are balanced to ensure proper weight distribution while being centrifuged. The four plastic jars are then inserted into four aluminum centrifuge cells.

The four balanced jars are placed into the high-speed refrigerated Fisher 21K centrifuge for 15 minutes, at a temperature of 4°C, and at a speed of 4700 rpm. The centrifugal forces of the

instrument pellet the bacteria to the bottom of the four plastic jars. The media broth floating above the bacteria is poured off, and the cells are placed in the freezer overnight.

The cells are stored overnight in the freezer for two reasons. First, protein degradation occurs rapidly and the bacteria must be cooled to slow all metabolic processes. Second, the freezing of cells, and the subsequent crystallization of water, helps break down bacterial cell membranes and makes the later lysing process more effective.

The frozen cells are lysed by a total of 40 mL of a Bacterial Protein Extraction Reagent, BPER, which is patented by Pierce Chemical Company. BPER is a non-ionic detergent solution that chemically lyses bacterial cells open for the purpose of subsequent protein extraction. The lysed bacteria and BPER solution are stirred into a homogenous solution, and then put into 28 mL centrifuge tubes. The tubes are then placed into a high-speed refrigerated centrifuge in a fixed-angle rotor and spun at 14,000 rpm for 15 minutes. The 2 liters of culture produced, on average, about 16 grams of bacterial cells.

Dialysis

After centrifugation, the insoluble parts of the bacterial cell are pelleted onto the bottom of the centrifugation tubes, and the protein aconitase is suspended in the solution. The clear, viscous protein laden solution is collected and placed into about 40 cm sterile dialysis tubing.

The tubing, which is made of cellulose, has pores of a specific size that retain molecules above a molecular weight cutoff (MWCO). Unwanted molecules, such as buffer agents, salts, and smaller proteins diffuse into a surrounding buffer solution. The Spectra/Por Membrane dialysis tubing used is made by Spectrum Laboratories and the MWCO is 25,000 kDa.

The dialysis tubing is then placed into a tall graduated cylinder filled with a 20mM Tris/.4M KCl buffer solution, pH balanced to 7.4. The protein/dialysis tubing must remain in the buffer solution for at least 4 hours in the cold room with continuous stirring, and the solution should be replaced at least once with fresh buffer.

At this point, the protein has been sufficiently separated from bacterial cellular components such as DNA, membranes, and metabolic products. However, the protein must be highly purified and isolated so that accurate characterization can take place.

Protein Purification

During the course of experimentation, the purification process became one of the most difficult problems to solve. The recombinant form of h-IRP1 used had a “histidine tag” consisting of six consecutive histidine residues attached to its amino-terminus (front end). The his-tag has been shown not to interfere with the function of h-IRP1 (Gray et al, 1993). The purpose of this tag is to allow the protein to be purified based on the affinity of histidine for nickel. Despite having a his-tag, it is still necessary to optimize the purification method.

Previous literature stated that a Ni-NTA column, or nickel attached to solid support, should be loaded with the lysate, and 5mM imidazole solution. When followed by a 50 mM imidazole solution, the procedure would be sufficient for purification. Imidazole resembles histidine and competes for the nickel on the column. The following summarizes the evolution of the purification method using the literature conditions as a starting point.

Gel Electrophoresis

After each different separation method was tried, the quality of separation was assessed by means of gel electrophoresis. Electrophoresis is based on the principle of charge migration ratio to particle mass. Using a cross-linked polyacrylamide gel, a protein sample is loaded and placed under a voltage. The protein moves through the polyacrylamide gel based on molecular weight.

More specifically, gel electrophoresis utilizes the detergent SDS (sodium dodecyl sulfate). SDS binds to most proteins in proportion to their molecular weight. The bound SDS gives the protein a large net negative charge. The gels, which also contain SDS, are loaded with the protein and placed under an electric potential. Because SDS separates the protein on the basis of molecular weight, larger proteins migrate more slowly and smaller proteins migrate faster. Therefore both protein purity and approximate molecular weight can be discerned. The position of the protein is determined by staining the clear gel blue with the dye Coomassie Blue.

When studying proteins using gel electrophoresis, an approximate molecular weight is the criteria of identification. By using a set of marker proteins, with known molecular weights, the mass of unknown proteins can be estimated. Using Precision Protein Standards, made by Bio-Rad, as markers for comparison in every gel run, a consistent basis for identifying a purified protein was possible. Below is a sample gel with the Precision Protein Standard and the associated proteins. The approximate molecular weight of aconitase is 98 kDa.

Figure 10 Guideline for Molecular Weight Migration

Purification Methods Development

First method:

a. load a column with 1 mL of Nickel resin (shown below):

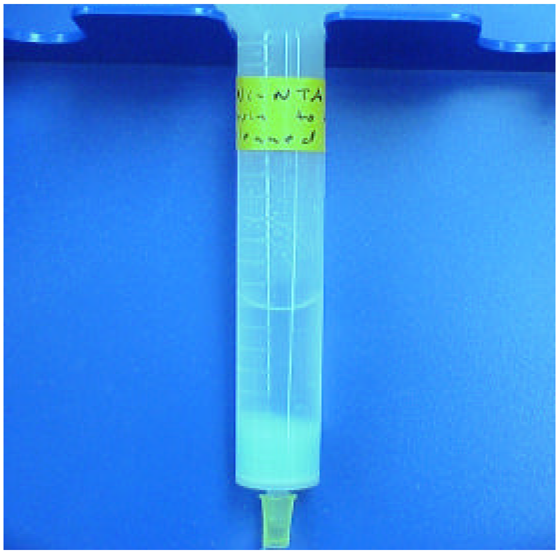

Figure 11 Ni-NTA column resin used first

b. Pour > 10 mL of 20mM Tris/.4M KCl buffer solution saved from dialysis into the column

c. Load lysate onto column. The Nickel column starts as a light blue color, but as protein is added, the color changes to a light brown.

d. The 5 mM imidazole is loaded and the eleunt solution that flows through the column and to the end of the column) is collected.

e. The 50 mM imidazole is loaded and the eleunt is collected. The aconitase protein should be found in this solution.

The following gels show bands of purified lysate. The top, dark band is where the protein was loaded into the gel. There are ten lanes of analyte. The far left is the marker strain, and the next four are 5 mM imidazole elutes, and the 5 remaining lanes are 50 mM imidazole elutes. Most of the protein, as well as impurities can be seen in lanes 3,4, and 5.

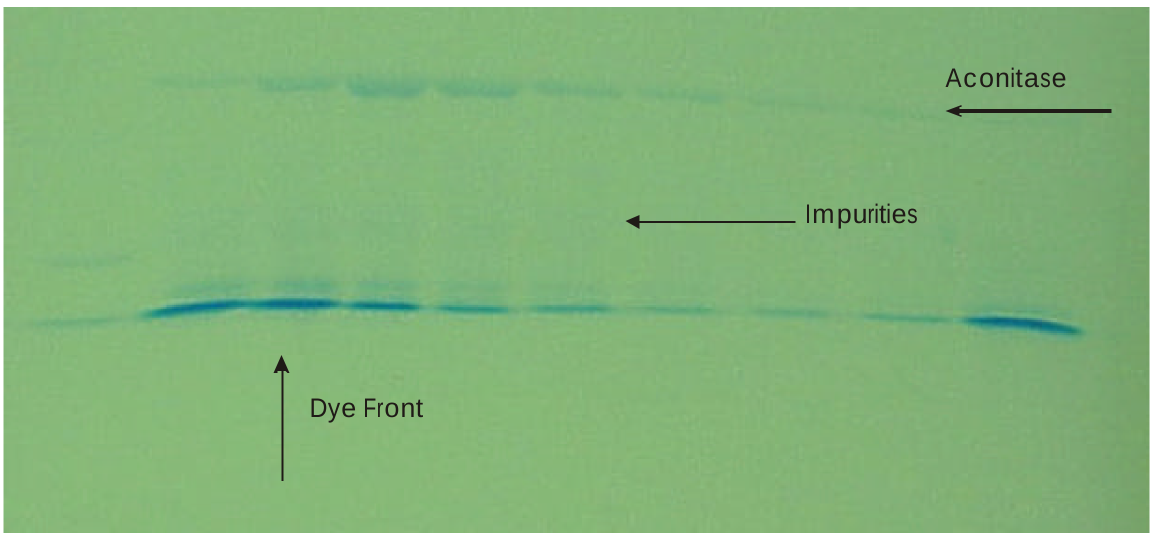

Figure 12 Initial gels show considerable impurity despite purifications steps

Column chromatography works by the principles of competition. At some point when using the 5 mM imidazole, the aconitase prematurely eluted off of the Ni-NTA column instead of waiting for the 50 mM solution.

Given the apparent impurities and lack of clear separation in the 5 mM and 50 mM solutions, the need for a concentration gradient became necessary. Therefore, an instrument

with a programmable concentration gradient was utilized. Shown below is the AKTA*prime*. The purpose of using this instrument was to obtain a more purified protein sample.

Figure 13 AKTA chromatography

The Amersham Pharmacia AKTA chromatograph was used to create an even concentration gradient beginning with 5 mM imidazole solution and ending with a 100 mM solution. The time period to develop the changing gradient was 20 minutes and samples of approximately 1 mL each were collected using an automated collection system.

From the AKTA chromatography, positive results were obtained. The 23rd through 30th vial had a brown tinge of color in the viscous solution, indicating the presence of aconitase. The aconitase protein has the iron-sulfur center, and because of the iron, the protein actually yields a light brown color to the solution it is in. Shown below is an example of the protein aconitase that has been purified and tested.

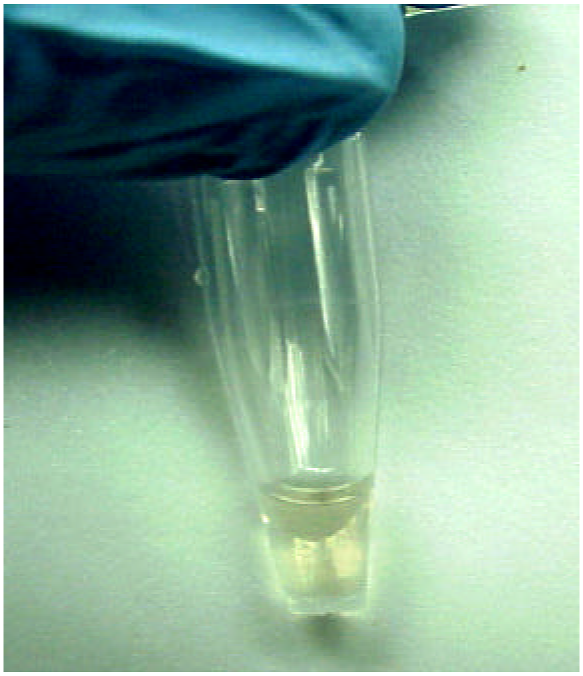

Figure 14 The light brown color of the aconitase protein is seen on the right in this vial of purified protein.

Based on the promising color of a discrete number of elution vials following the revised chromatography technique, another gel was run to assess the aconitase purity. The following two gels show a broad range of elution vials tested. Vials number 5, 10, 15, and 20 showed no signs of brown color, and they were tested as a precaution. Vials 23-30 were tested, and these vials showed the significant brown coloration. Finally, vials 35, 40, and 45 were tested as a precaution again in case the aconitase had not been responsible for the brown color and had in fact eluted into other vials. Shown below are the two gels.

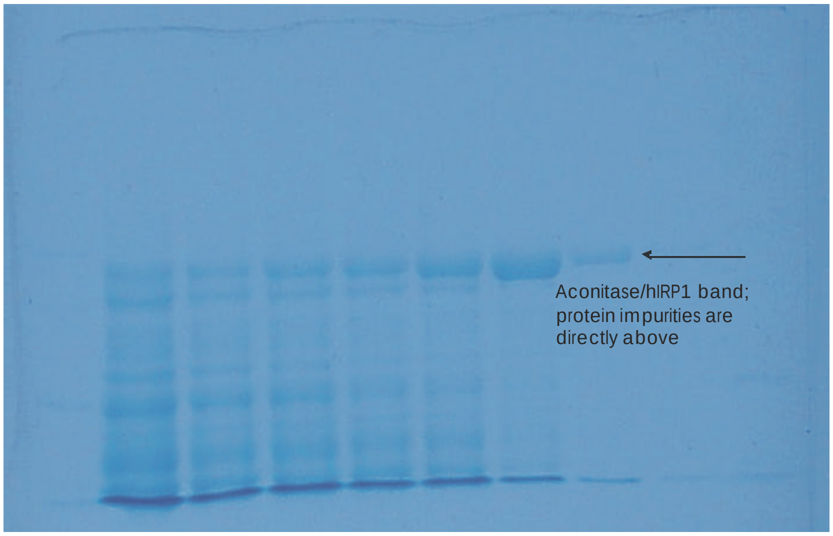

Figure 15 The above arrow shows the bands of protein impurities that lie between the top hIRP-1 band and the dark dye front lining the bottom of the gel.

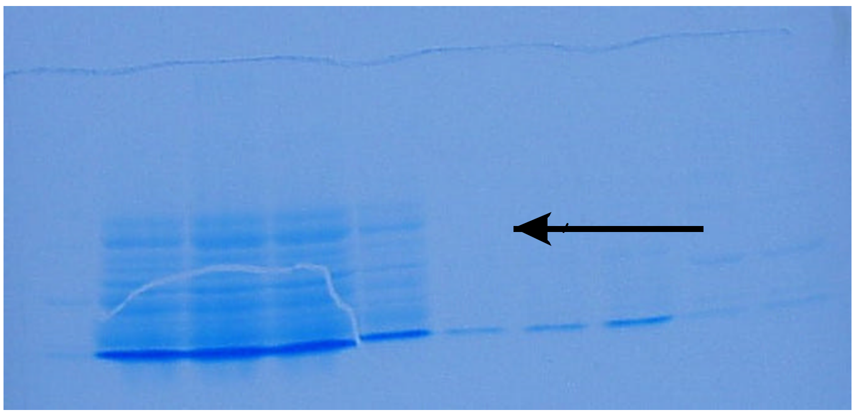

Figure 16 The above arrow shows again the impurities found in the purified protein sample. The top of the gel is the hIRP-1 protein, and the dark blue line on the bottom is the dye front.

Large amounts of aconitase are present in the sample, as shown in the above two gels, and the heavy bands of blue stain once again indicate a high level of impurity. As before, when only the Ni-NTA column was used, the fractions containing aconitase was still contaminated with other proteins. The persistent presence of similar looking bands, with the use of procedures from chemical literature, leads to the following conclusion and modification of procedure.

The protein, after being lysed with BPER, is surrounded by large amounts of cellular components. One of the components includes proteases. A protease is an enzymatic scissor designed to cut a protein in specific places on the basis of structure and contribute to the metabolic cycles of synthesis and degradation.

The aconitase protein being synthesized and purified for this research project is extraordinarily sensitive to the effects of proteases. Though a portion of aconitase protein is degraded by a protease, the histidine tag remains with these fragments. When the histidine tag of aconitase is eluted, these fragments elute as well.

Several controls were implemented to alleviate the degradation. First, time is a critical factor and all dead time between lysing, centrifugation, and subsequent purification was minimized. As laboratory proficiency was gained over the course of the project, protein preparatory time was reduced from about ten days to a total of about three days.

Second, all steps were modified and performed over ice. The cooler temperatures slow down cell activity and help to inhibit proteasome degradation. Conscientious precautions were taken throughout all experimentation to ensure the protein remained over ice and that minimal degradation occurred.

Finally, a chemical inhibitor was added. The chemical phenylmethylsulfonylfluoride (PMSF) is added in small amounts before chemically lysing the cells. The PMSF preferentially binds to the proteases and prevents degradation of the aconitase.

Biochemical systems demonstrate greater sensitivity to ambient conditions such as time, temperature, and oxygen exposure. Among the most important modifications to experimental protocol made throughout the year were heightened awareness to sterility precautions and to time elapsed between purification steps.

Development of the Enzyme Assay

Immediately after a purified sample is obtained and verified, enzyme assays must be run in order to discern both whether the protein is the one intended on being over-expressed and harvested and if the protein is enzymatically active. The assay we originally attempted to use in the biophysical characterization of aconitase was a coupled assay following the UV signal obtained from creation of NADPH.

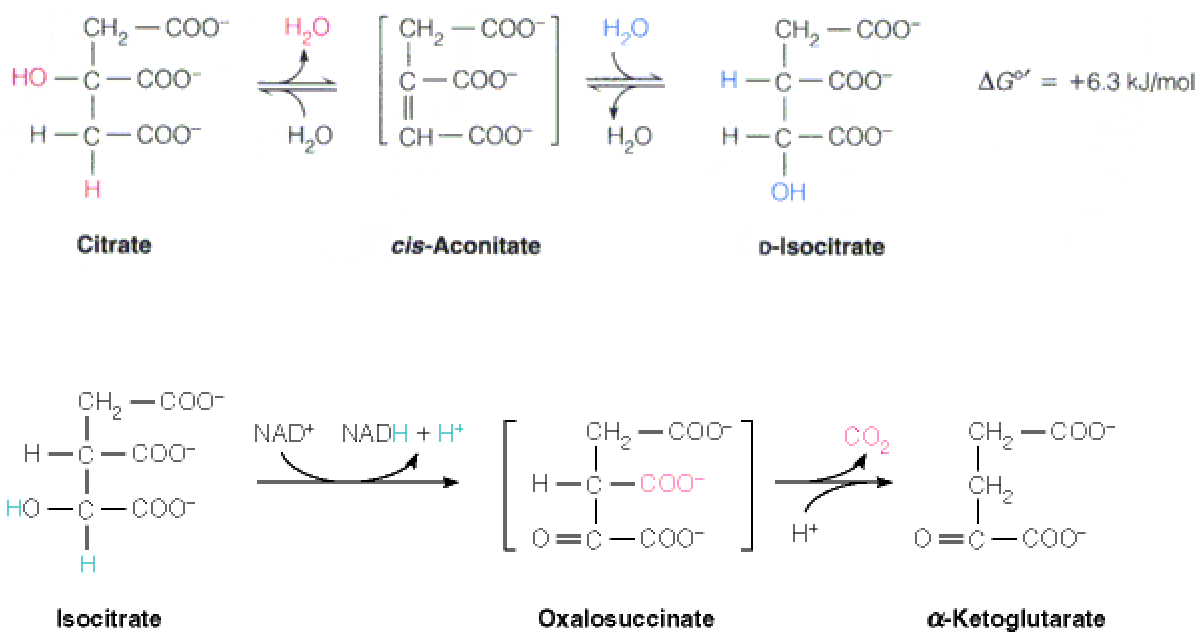

Figure 17 The above two reactions represent two successive steps in the Kreb's cycle, the main metabolic pathway in the human body. In the coupled assay, the production of oxalosuccinate, as monitored by the production of NADPH, indicates the activity of the aconitase enzyme, which catalyzed the top reaction. (**http://www.awl.com/mathews/ch14/frames.htm**)

Control runs of the assays were first conducted on samples of purified porcine heart aconitase obtained from Sigma Chemical. After human aconitase samples were produced, similar

assays were run to ascertain activity. Essentially, a rise in absorbance at 340 nm should be observed, and the absorbance should increase with respect to time as the reagents react.

Despite repeated attempts, obtaining a change in absorbance graphically remained elusive. According to literature procedures, 90-minute (Rose& O'Connell, 1967) observation periods were conducted and linear enzyme activity was observed. However, in our lab, no significant changes in activity were observed.

Several modifications were attempted to possibly produce an increase in observed absorption. First, enzyme volumes were adjusted. By increasing the amount of aconitase, isocitrate dehydrogenase, and $NADP^+$, more of a reaction might be possibly observed. Despite these modifications, no significant increases in absorbencies were obtained.

Then, small amounts of low concentration iron sulfate and sodium sulfide were added to the purified protein as a means of activating the protein. The h-IRP is the purified protein, and additions of iron and sulfur species must be provided to induce cluster assembly.

The excess iron sulfate and sodium sulfide were filtered away to ensure these two species would not reduce the $NADP^+$ and cause a false change in absorbance. However, the activated protein showed no significant changes in absorbance at 340 nm.

Another modification included adding an excess of enzyme. 50 µL of activated aconitase were added to the complete enzyme assay. A change of almost 100% in absorbance at 340 nm occurred, though no linear change with respect to time was obtained. At this point, fast kinetics became a distinct possibility.

Next, enzyme assays using a sample of inactivated protein was conducted. The use of inactivated protein was in fact a control step against residual iron sulfate and sodium sulfide being the source of absorbance changes.

For reasons unknown, the coupled assay never worked in our hands. Therefore, experimental efforts were redirected to the development of a simpler, more direct assay, described below.

Direct Assay

Numerous attempts to successfully gain meaningful results from the coupled assay remained elusive. After consulting the literature again, the assay used to determine h-IRP activity and identity was changed to a direct assay (Drapier &Hibbs,1986).

Instead of relying on a complex, two step reaction with concerns regarding reversibility of enzymes, reagent concentrations, and competing reactions, a direct assay provided a much more clear and controlled method of measuring activity. Advantages of the direct assay include prevention of isocitrate formation, which could interfere with subsequent activity experiments. Also, any unreduced Fe(II) still in the protein solution could potentially be reduced and increase NADPH signals falsely.

A final advantage of the direct assay is that it would allow enzyme activity to be used as a measure of the native state of aconitase alone. In the coupled assay, it would be difficult to know whether denaturants were affecting the aconitase, isocitrate dehydrogenase, or both enzymes.

The direct assay used is citrate isomerization assay as shown below.

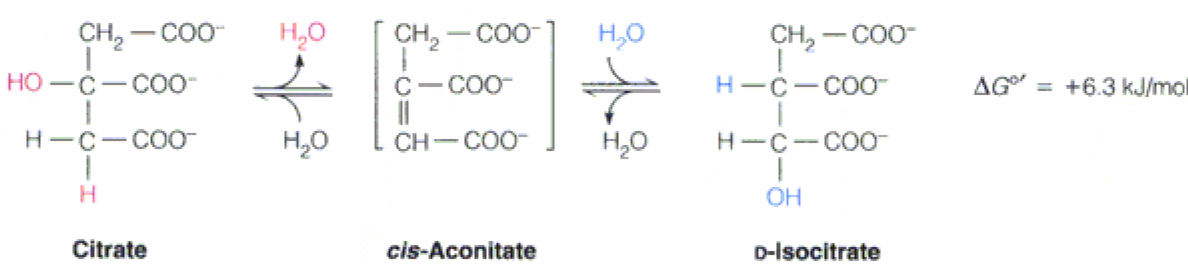

Figure 18 Enzymatic reaction of the direct assay

Citrate, *cis*-aconitate and d-isocitrate all absorb light in the UV-Vis region, a fact which was confirmed experimentally using a Hewlard-Packard 8452 Diode UV-Vis Diode Array Spectrophotometer.

The maximum absorbance of *cis*-aconitate was determined to be 240 nm and isocitrate was 212 nm. The preponderance of *cis*-aconitate concentration versus the formation of isocitrate concentration made tracking a decrease in *cis*-aconitate a better assay as the formation of isocitrate was catalyzed by the purified and activated aconitase. Evidence of activity was successfully monitored using a Gilford Response UV-Vis Spectrometer, as shown below.

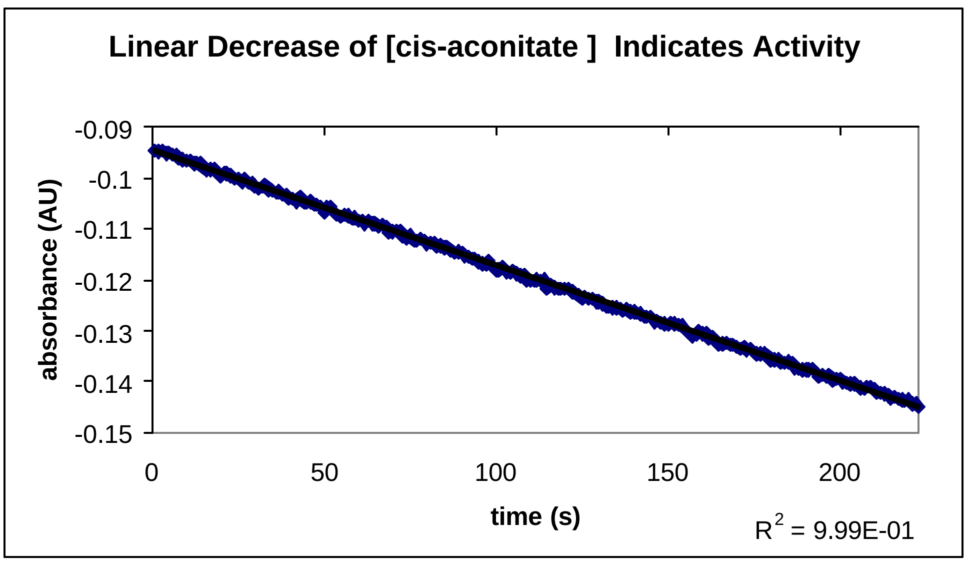

Graph 1 The above graph shows a linear decrease of *cis*-aconitate concentration as observed at 240 nm. The assay follows the consumption of *cis*-aconitate as a measurement of aconitase activity.

III. Experimental Results

Initial Unfolding Studies

After confirming both enzyme purity and activity, characterization studies began. A myriad of methods and instrumentation can be employed to perform characterization studies. Among the methods proposed were thermal denaturation and chemical denaturation, both of which can be monitored using enzymatic assays, visible and ultraviolet spectroscopy, and fluorescent spectroscopy.

After the synthesis and purification of the aconitase enzyme, the enzyme concentration was low, effectively limiting the usefulness of visible and ultraviolet spectroscopy.

Instead, fluorescence was chosen as the main spectroscopic method. Fluorescence is an extremely sensitive analytical tool, and a strong intensity signal was obtainable despite the low concentration of pure aconitase enzyme.

The fluorescence method takes advantage of different energy configurations in both the native and unfolded state. As a general analytical assumption, fluorescence generally decreases after denaturation because previously buried side chains in the native state protein are exposed to solvent.

After fluorescence was chosen as the method, a concentration of 6.48 M urea-denatured aconitase was used to set initial conditions for more refined experimentation. The use of such a concentration of urea ensured the complete unfolding of the aconitase. When the samples of freshly purified protein were subjected to the high concentrations of urea, an unexpected, yet significant, increase in fluorescence occurred.

This experimental observation carried numerous implications regarding protein structure and unfolding mechanisms. An explanation of both chemical denaturing and fluorescence is

essential for understanding the principles behind many of the experimental conclusions that follow.

Theory of Chemical Denaturation

Chemical denaturation is an analytical tool for the study of proteins, providing information on conformational stability, unfolding mechanisms, and structural features. The conformational stability derived from the denaturation curve essentially describes how much more stable the native, folded state is than the unfolded, denatured form. A denaturation curve also gives insight into the folding mechanism by revealing if an unfolding mechanism is either a two-state conversion between native and denatured states or a multiple-state mechanism involving intermediate states.

As a protein is subjected to chemical unfolding using either urea or guanidine hydrochloride, GdnHCl, most physical properties of a folded protein change. Numerous analytical techniques to observe the physical changes are available including UV spectroscopy, circular dichroism (CD), NMR, and fluorescence (Finn et al, 1992).

Fluorescence lends itself particularly well to the study of protein folding because several amino acid residues possess an intrinsic fluorescence. For most proteins, protein in its native state fluoresces more than an unfolded, denatured protein. Three amino acids, tyrosine, tryptophan, and phenylalanine all exhibit fluorescence.

Theory of Fluorescence

The majority of spectroscopic techniques track a spontaneous radiative decay process. A radiative decay process begins with the initial excitation of an electron into a higher, excited

energy level. As the excited electron decays, the absorbed photon is emitted at a distinctive wavelength and various spectroscopic techniques can observe this emission.

Fluorescence decay is a unique process and differs significantly from normal electronic decay. Like electronic decay, a given molecule is taken to an excited state after initial absorption. After the absorption, the upper vibrational states undergo radiationless decay by giving up energy to the surroundings. A radiative transition then occurs from the vibrational ground state of the upper electronic state. (Atkins, 503)

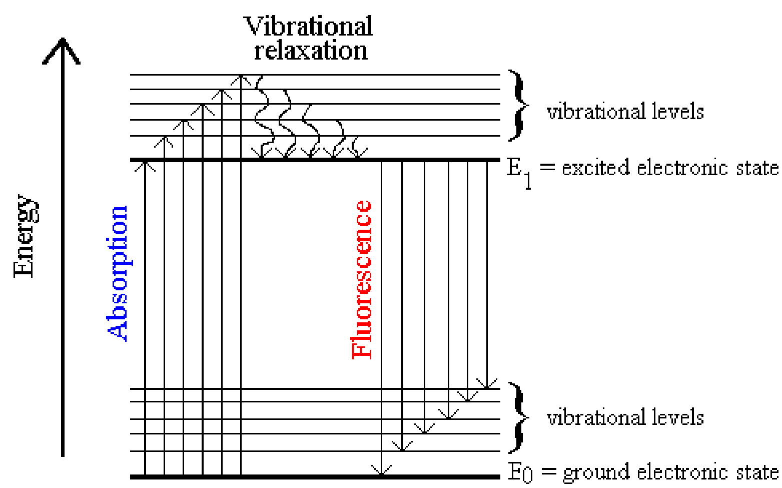

Figure 19 The energy levels of molecules all contain numerous vibrational and rotational levels, and energy can descend within a given electronic state in these vibrational and rotational states.
http://lc.chem.ecu.edu/Class/Mathis/2251/FL.htm

The three amino acids that exhibit fluorescence all contain a six-sided ring structure, and it is this structural feature that gives the fluorescence.

Shown below are the three amino acid residues that fluoresce. Of the three, phenylalanine is the weakest fluorophore due to the least amount of ring structure. The ring structure allows for a binding phenomena known as conjugated systems to form, and the conjugation allows for increased structural rigidity and subsequent reduction of energy loss by internal conversion. (http://pps99-1.cryst.bbk.ac.uk/projects/gmocz/fluor.htm)

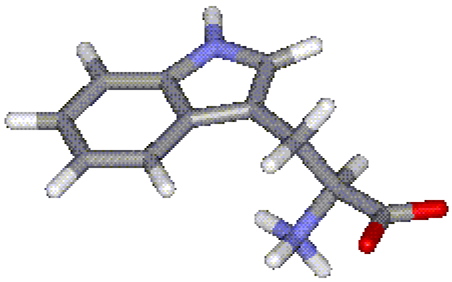

Figure 20 **Tryptophan-** Of the three amino acids, tryptophan has the strongest fluorescent signal because of its extensive ring system. The best wavelength for observation is at 295 nm

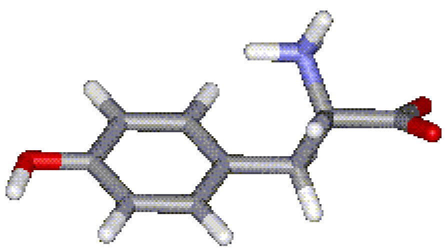

Figure 21 **Tyrosine**- Tyrosine also exhibits a fluorescent signal, though significantly less than tryptophan. The optimal wavelength for observation is 280 nm.

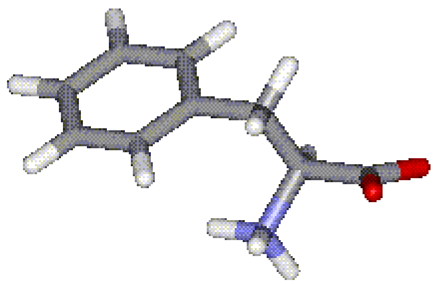

Figure 22 **Phenylalanine** – The weakest of three amino acids, phenylalanine's signal was not followed for this projects characterization studies

As described before, fluorescing amino acids all contain 6-carbon ring structures, and they gain increased structural rigidity from a bonding concept known as conjugation. Conjugation allows electron density to be de-localized over unhybridized ? -orbitals.

An interesting phenomenon occurs when these three amino acids are in relatively close position and interact accordingly. The conjugated Π- bonding of each residue shares electron density with the other residue's conjugated system. The shared electron density actually results in lower electronic energy and decreases fluorescent signals of the folded, native state globular protein. This lowering of the folded state fluorescence is known as quenching.

In proteins that quench in the native state, electronic density is shared by the aromatic structure of two fluorescent amino acids. Therefore, the fluorescence increases as the protein unfolds due to a relief of quenching as the amino acids move apart.

Initial Fluorescence Results

Initial additions of urea revealed an increase in fluorescence.

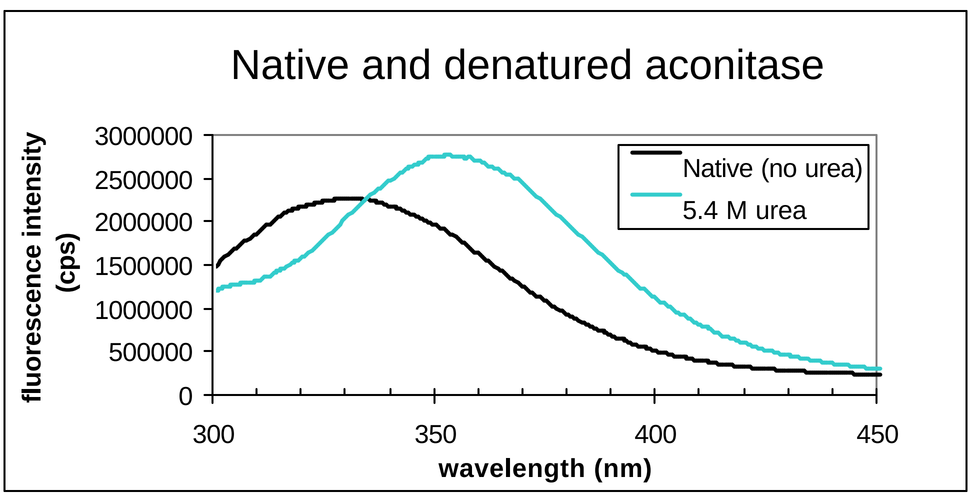

Graph 2 Maximum difference between folded and unfolded state is 370 nm

The experiment was designed to excite the aromatic structures at 295 nm and then collect an emission scan over a range of 300 to 450 nm by using a Spex Fluorolog-3 Fluorometer. This range of emission is in both the ultraviolet and visible spectrum. As seen in the above data, activated aconitase shows both a red shift due to solvent absorption *and* an increase in fluorescence between folded and completely unfolded states.

Based on initial observations of the native and denatured states, the significant change in fluorescence magnitude suggests several phenomena that can be exploited in further investigations. First, as stated before, quenching of aromatic residues is possibly present and can account for the increase in fluorescence. Second, the magnitude of intensity changes suggest the fluorescing residues are buried deep within the hydrophobic environment and away from energy absorbing effects of solvent. Without a solved crystal structure, such an effect could not have been predicted.

Central Problem of Proteomics

With the conclusion of the human genome project in 2000, the next herculean task entailed correlating proteins with specific genes. Proteomics is the name given to this area of research. The goal of proteomics is to obtain a complete understanding of both mechanism and structure for all products of the genetic code.

In the case of h-IRP1/*c*-aconitse, the linear genetic sequence of amino acids has been solved, but to date, a three- dimensional structure has not been determined. The h-IRP1/c-aconitase protein is a large monomeric protein with multiple domains, and the complexity of both its structure and function add to the overall challenge in performing protein-folding studies.

Without a three-dimensional structure, conclusions regarding quenching can be hard to reach. However, its functional analogue, porcine mitochondrial aconitase, does have a solved three-dimensional crystal structure. Extensive analysis of the sequence homology has been performed, and the assumption that h-IRP1 resembles porcine mitochondrial aconitase has been made (Kaldy, 1999). Based on alignment of the porcine mitochondrial aconitase and human cytoplasmic aconitase, a hypothetical model for the c-aconitase was using Swiss Prot Viewer analysis software. More tryptophans are present in the human cytoplasmic aconitase, and these tryptophans were substituted into the porcine mitochondrial aconitase in places where the two sequences lined up.

Inspection of the hypothetically modeled structure revealed that two trytophans, Trp 129 and Trp 527 in the human cytoplasmic aconitase, are positioned in such a manner as to allow quenching. The two diagrams below show the hypothetical model and a close view of the proposed quenching.

Structure of Aconitase

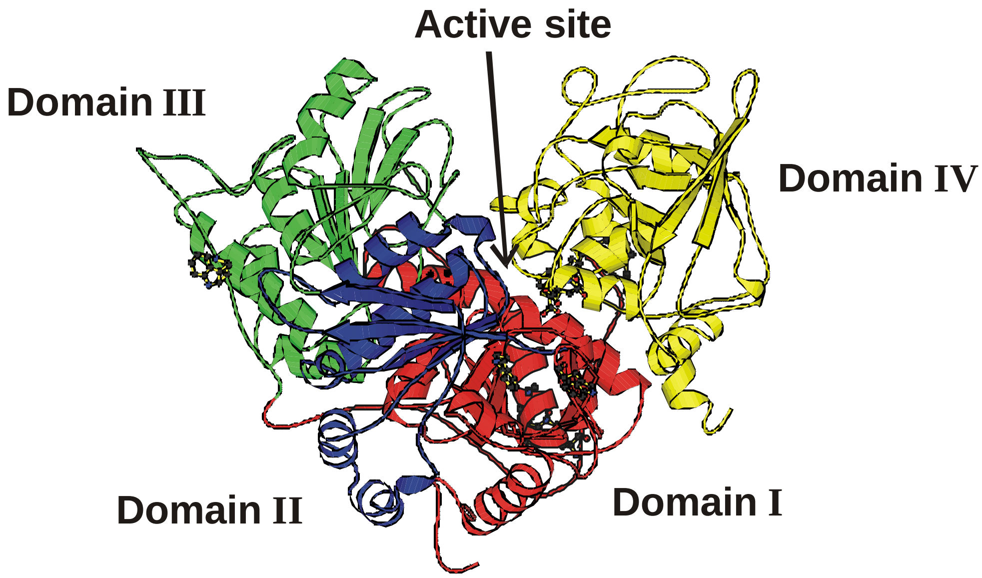

The seven tryptophans from the human version of cytoplasmic aconitase have been modelled into the structure for porcine heart aconitase (PDB code 6ACN) based on sequence alignment.

Figure 23

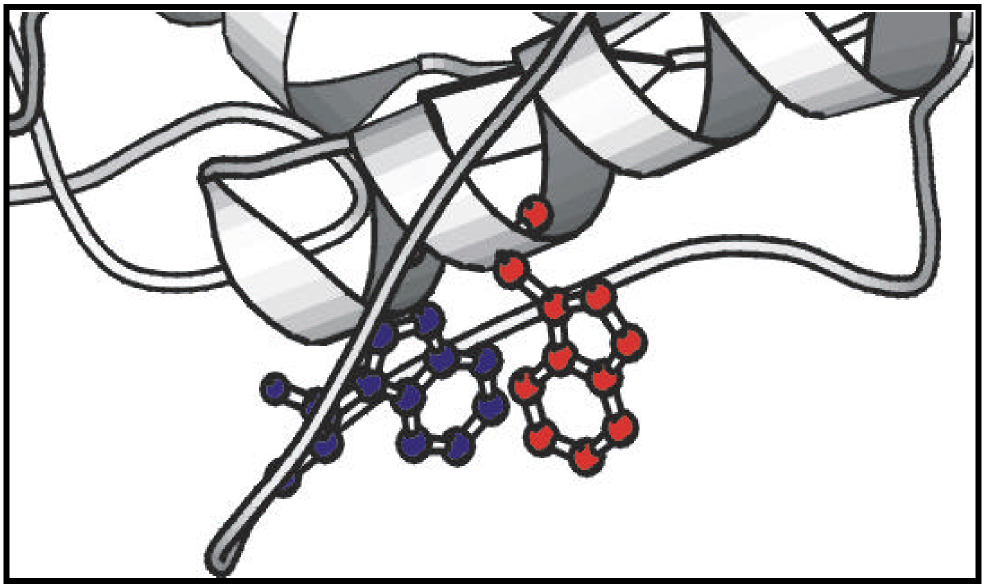

Figure 24 This segment of the fourth and first domain clearly shows the two substituted tryptophans. Trp 129 is the lighter residue, and Trp 527 is the darker residue. Their distance and orientation contributes to exciton coupling and a quenching of fluorescence.

Experiments were designed to test the possibilities that these residues were causing the unusual fluorescent result. Porcine mitochondrial aconitase, from Sigma Chemical Company, was purified by ion exchange chromatography on the AKTA instrument and subjected to the same denaturation as the prepared cytoplasmic aconitase. The purpose of performing chemical denaturation on the porcine heart aconitase was to support the hypothetical quenching model. The porcine aconitase does not have the two tryptophan residues at 129 and 527, therefore, a decrease in fluorescence was predicted as the protein unfolded.

Samples of porcine aconitase were prepared with urea concentrations ranging form 0 M to 5.4 M. After being allowed to equilibrate overnight, the samples were sequentially scanned for both the spectrum and for intensity at 370 nm. Using the Spex Fluorolog-3 Fluorometer, spectra were collected at an emission range of 300 nm to 450 nm after exciting at both 280 nm and 295 nm.

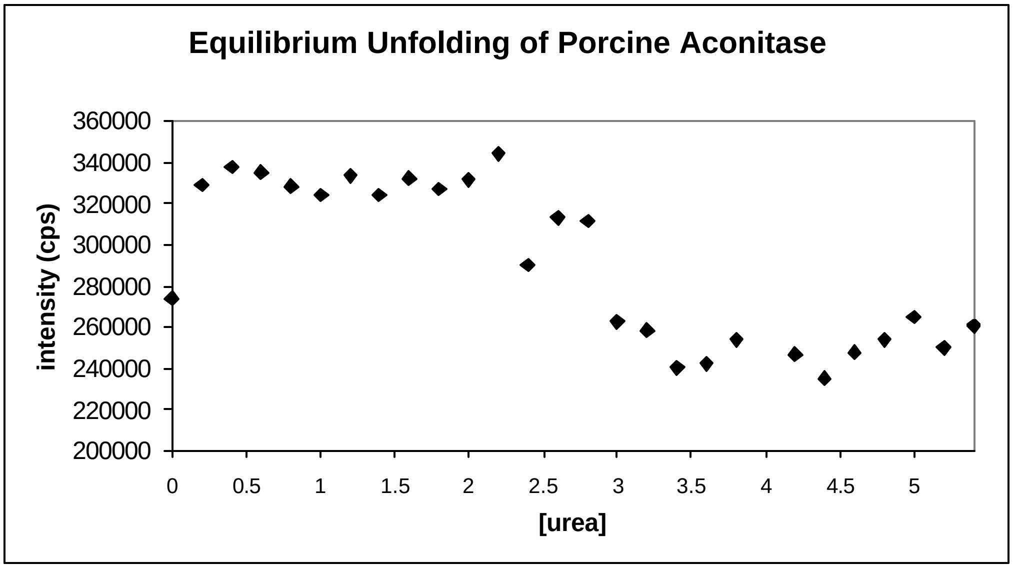

Graph 3 Decrease in Fluorescence of Unfolded state for Pig Heart Aconitase observed, inline with Trp quenching theory. The urea samples were excited at 295 nm and an emission intensity at 370 nm was collected.

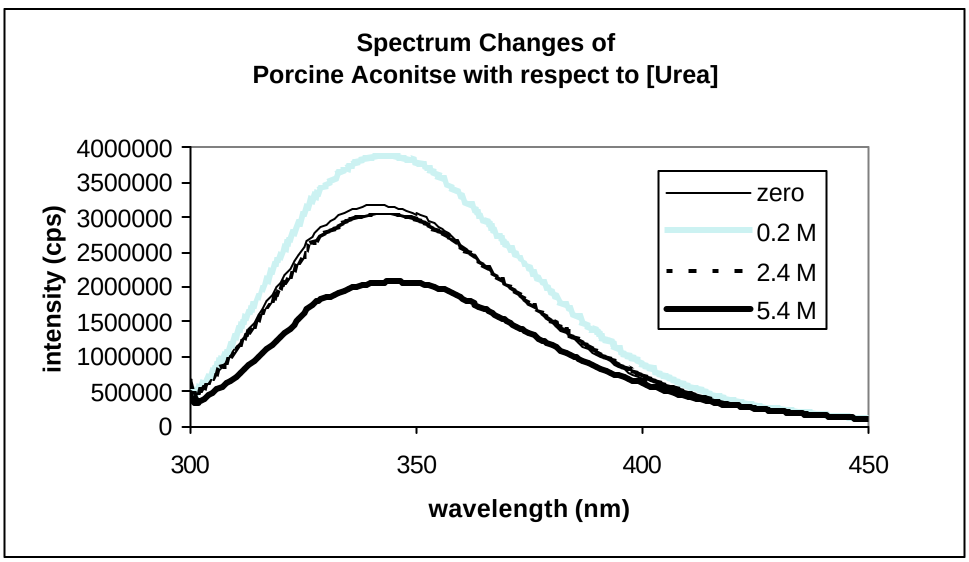

Graph 4 Little red shift is observed in the denaturation of porcine *m*-aconitase; however, decreased fluorescence is observed in the fully unfolded 5.4 M [urea] sample

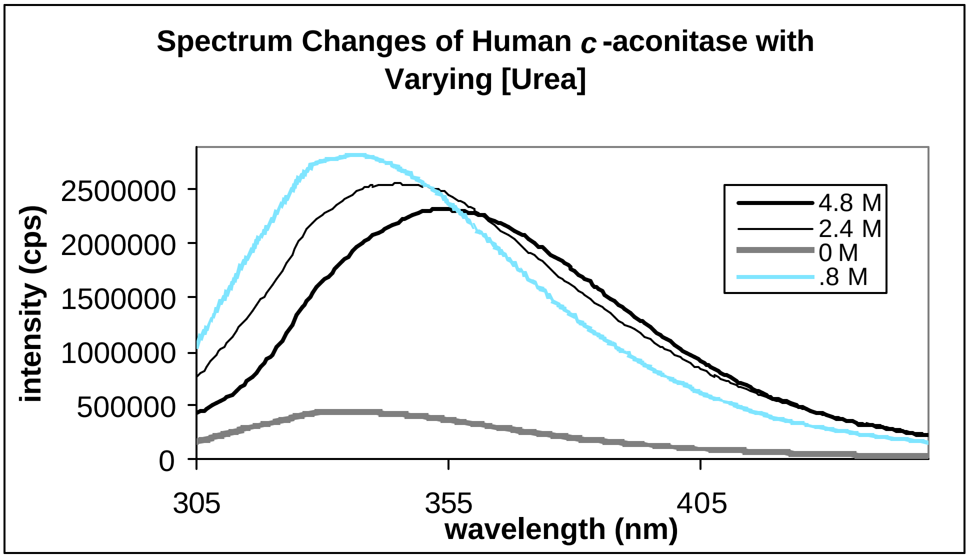

Graph 5 In contrast, *c*-aconitase shows signicant red shift and increased fluorescence of the denatured state

Structural and Functional Homology

Linear sequences of amino acid residues can be obtained from PUBMED, an online, international database of biochemical data (www.ncbi.n/m.nih.gov). After finding desired sequences, online software is also available which can compare such linear sequences and determine percent identities between any two proteins (Person et al, 1997).

Protein	# Of Residues
Human c-aconitase	889
Human *m*-aconitase	747
Pig *m*-aconitase	754

Figure 25 Shown above are three analogous protein structures and the number of amino acid residues coding for each protein

Genetic Sequence	**Percent Identity (%)**
c-aconitase and m-aconitase	27.0 %
m-aconitase and pig m-aconitase	95.9 %
c-aconitase and pig m-aconitase	26.7 %

Figure 26 The amino acid sequence for the three analogous proteins were compared to one another for identity of sequencing residues.

The conclusions of the alignment study are revealing and enigmatic. Two enzymes within the body, the cytoplasmic and mitochondrial aconitase share the same enzymatic activity and are from the same species, and yet only share 27% similarity in their genetic sequence. Corresponding to the lack of structural identity between the two species is the fact that the two enzymes originate from two different chromosomes.

Interestingly enough, the porcine and human mitochondrial aconitase share nearly 96% identity, and this high percentage suggests a strong evolutionary preservation of a highly successful iron-sulfur enzyme.

The percent identity between pig mitochondrial aconitase and human cytoplasmic aconitase is rather low considering the above two relationships.

Though apparently low at 27%, the structural similarities between mitochondrial aconitase and cytosolic aconitase are strong enough to permit assumption of structural homology. (Kaldy, 1999)

Unfolding Mechanisms

Based on the easily tracked fluorescent signal of c-aconitase, studies were performed to probe the unfolding mechanisms.

First, a determination of where maximum wavelength differences occur between folded, native state and unfolded, denatured state was made by subtracting spectra taken in the two states (see graph 6).

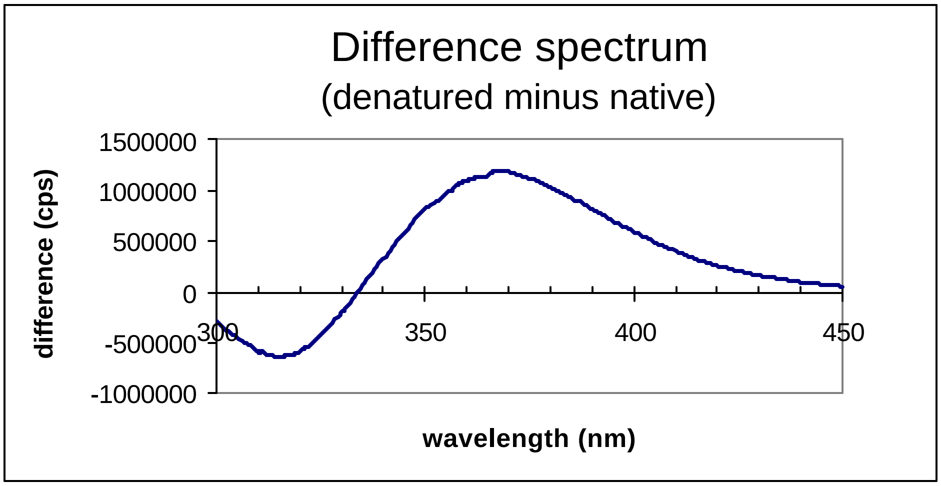

Graph 6 Maximum Difference is obtained at 370 nm between folded and completely unfolded states of aconitase

As shown in the graph above, differences between the folded and unfolded state emission spectrum were plotted and the max difference was determined to be 370 nm. After the determination of this characteristic wavelength, experiments were constructed to follow this wavelength.

The first question to be experimentally probed sought to derive a correlation between denaturation and loss of activity. Essentially, the experiment was designed to figure out how important structure was to the enzyme's ability to work properly. This experiment also seeks to discern how much denaturing stress the aconitase can handle while still functioning.

A series of aconitase samples were prepared ranging from 0 M urea to 5.4 M. Using a spreadsheet to determine volumes of each reagent, each sample had a final volume of 400 µL. A

standard addition of 100 μL was added to each sample to ensure uniform intensity signal. A 50 mM Tris buffer and 9.5 M stock solution of urea were used to make the range of samples.

Next, fluorescence data over the range of samples was collected. Interesting conclusions of these scans revealed a multi-step equilibrium process for unfolding. As urea concentrations increased, and increased unfolding ensued, fluorescence at 370 nm increased. The maximum difference between native and unfolded state is at 370 nm, and the derivation was described before. As seen in the experimental data, at least three intermediates are present as the protein unfolds indicating a multiple-step equilibrium mechanism for unfolding, as shown below.

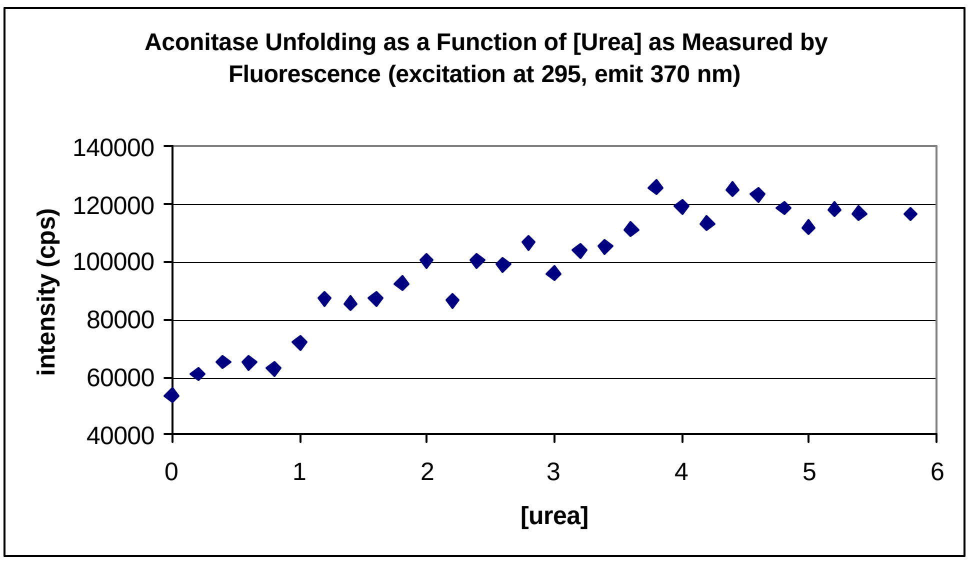

Graph 7 Before the final unfolded equilibrium is reached, three intermediate equilibriums states are observed.

The presence of multiple equilibria leads to several questions. First, where in the denaturation process does aconitase lose its activity? Second, are the equilibrium plateaus a result of iron-sulfur cluster disruption or perhaps structural conversion from the enzyme aconitase to the genetic regulator h-IRP1? Finally, the plateaus can also be a result of the four domains of the monomeric protein becoming unfolded as regions. It is possible that one region

could be more unstable than another, or perhaps the domains confer some sort of protection to one another.

The samples prepared for the fluorescent scans were also used to test activity. The same assay procedures utilized to confirm enzymatic activity of the purified h-IRP1 were applied to the range of denatured samples. Based on observed activity, and corresponding normalized slope, a loss of enzymatic activity was observed at a [Urea] of 2.4 M, as shown below. By 2.4 M, no activity was detected.

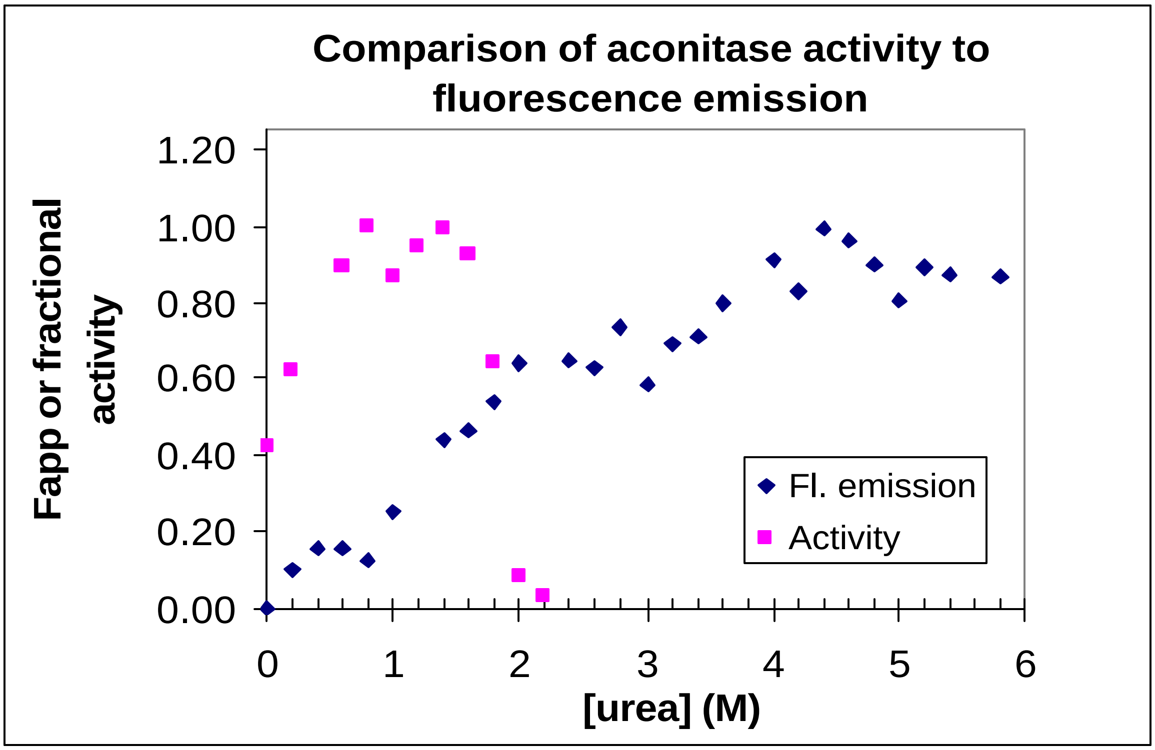

Graph 8 A correlation between intermediate equilibriums and activity is observed. Following initial increases in activity, at 2.4 M [urea] activity is abruptly lost

The initial additions of urea result in a notable increase in activity. This increase suggests two informative possibilities for the structural relevance. First, the active site of the aconitase is most definitely the iron-sulfur center. However, the fourth domain clamps tightly over the

binding site, allowing for limited activity. (Kaldy 1999) The fourth domain acts as a hinge, and with the urea effects, the clamp like effect decreases and activity correspondingly increases.

With the addition of denaturant, yet the overall protein integrity preserved, flexibility of the active site and relaxation of the fourth domain allow greater accessibility for the substrate and enzyme complex to form and for the product to be released. This is similar to an observation for the enzyme dihydrofolate reductase (DHFR) isolated from chickens, in which it was determined that urea made the enzyme more active because the flexibility of the protein increased, allowing faster turnover (Fan et al, 1996).

The above correlation between activity and structural changes is that a loss of activity appears to occur at the start of the second plateau. This second equilibrium suggests either a loss of the cluster or perhaps only the loss of the labile Fe in the cluster, leaving an enzymatically inactive 3Fe-4S center still bound by cysteine residues in the active site.

Experiments were attempted to determine the exact fate of the Fe-S center during the denaturing process. Using a method called electron paramagnetic resonance spectroscopy (EPR), the disassembly of the cluster could have been clarified on the principle of high spin and low spin states (Ebsworth, 1991). The 4Fe-4S state would have a high state spin based on its characteristic electron pairing, but the 3Fe-4S would have had a low spin from its characteristic pairing. Due to the low aconitase concentration, no signal was obtained.

Based on this data, the final state might represent unfolding of the protein scaffolding that remains intact after loss of the cluster or activity. Because the protein is bifunctional, a multiple step unfolding process seems reasonable. With the loss of the iron-sulfur cluster, the remaining aconitase structure must possess enough stability to assume its role as an IRE binding element.

Without the iron-sulfur center, the protein assumes its other function and must be able to function as an IRE regulation protein. For the scope of this investigation, ability to function as an IRP was not determined experimentally. However, the iron-sulfur center was removed and effects on protein structure were examined.

EDTA (ethylenediaminetetraacetic acid), a chelating agent, was added to a prepared sample of pure, activated aconitase. A chelating agent will have a higher affinity for a given species, in this case iron, and will preferentially strip that species from its host.

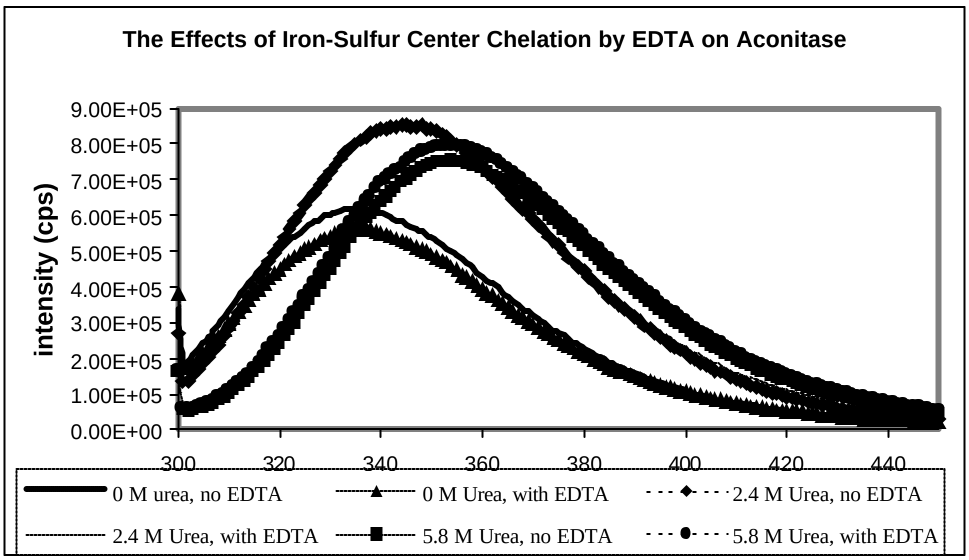

Graph 9 Spectra obtained from three urea concentrations in the presence and absence of EDTA are compared. Similar red shift and increasing fluorescence is observed regardless of cluster presence

Despite a lack of the active site metal cluster, there is no effect on the wavelength of maximum intensity (λ_{max}) between samples with and without EDTA additions. The red shift is present due to previously hidden residues being exposed to an aqueous environment. This suggests similarities regarding both structural integrity and final unfolded states in the presence and absence of the cluster.

With the loss of the iron-sulfur center, an interesting structural change occurred. In the native state, the fluorescence intensity is decreased in the presence of a molar excess of EDTA. However, at high urea concentrations, the intensity is increased in the presence of EDTA. At the point of previously determined loss of activity, 2.4 M [Urea], the intensity of both the native state and stripped enzyme are identical. Further investigation is required to determine the significance of these results.

Determination of Thermodynamic Stability

The general proposal for this Trident project included a determination of thermodynamic stability. Essentially, purified aconitase would be subjected to incremental changes in temperature. As the temperature increased, native state proteins would become denatured, or unfolded, and a stability curve could be constructed as a plot of temperature versus percent unfolded protein. The equilibrium of a protein exists effectively between two states, unfolded and folded; and, the equilibrium can be molded as such.

$$\boxed{\mathbf{F\ ?\ \ U}}$$

The relationship between the native state and the unfolded state can be represented by equilibrium constant, as shown below:

$$\mathbf{K_{eq} = [U]/[F]}$$

The unfolding mechanism itself does not influence the K_{eq} because the folded and unfolded states are independent of the pathway. Being independent of path, this mechanism is known as a state function, relying only on initial and final conditions.

After constructing an experimental curve of temperature, a curve using reiterative approaches can be fitted, and from the best fit curve, information concerning enthalpy, specific heat capacity, and stability can be derived. A non-linear least squares program named Savuka version 5.1, written by Lambright and Bilsel and available online, was used to perform data fitting analysis. The use of the online software was kindly allowed through the University of Massachusetts Medical School, Prof Robert Matthews Laboratory.

The thermal denaturation was performed with the use of a Peltier, a programmable thermoelectric temperature control attached to the fluorometer. This instrument allowed accurate thermal conditions to be maintained. After temperature equilibration on samples of 350 µL, the detector monitored the folded state of the protein as reported by the three fluorescent amino acid residues phenylalanine, tyrosine, and tryptophan.

Graph 9 illustrates the entire spectrum for aconitase, and as the temperature denaturation is applied, the intensity and shape of the curve changes. The least fluorescence, without any significant distortion of curve shape, occurs at 37ºC. In fact, normal body temperature is 37ºC, and the most stable temperature for a human protein would be at this temperature.

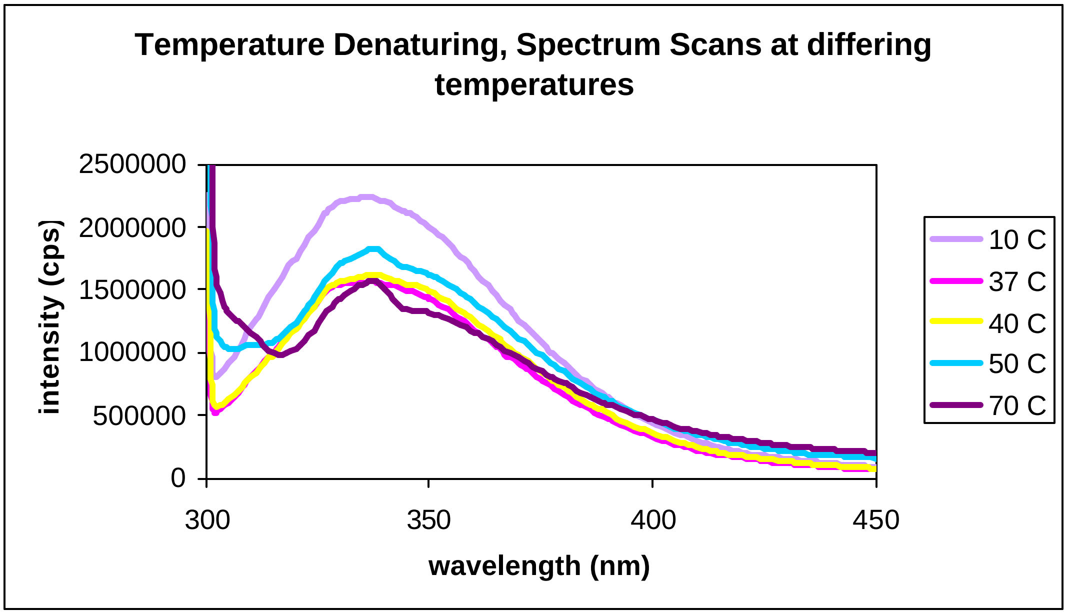

Graph 10 The above graph shows how the aconitase UV spectrum changes with addition of thermal denaturation

Graph 10, below, shows how the intensity varies at each experimental temperature at the wavelength 370 nm. The maximum wavelength difference between folded and unfolded states was determined earlier when chemical denaturation was applied, and the same wavelength was used for thermal tests.

Graph 10 clearly demonstrates the most favored, stable temperature occurs between 37-40ºC, and in fact, the data deviates slightly from the fit applied. At this critical range of temperatures, the protein might have some internal sense of resisting temperatures. However, the deviation was noticed on all sets of thermal data and possibly demonstrates the unique and narrow range of physiological homeostasis.

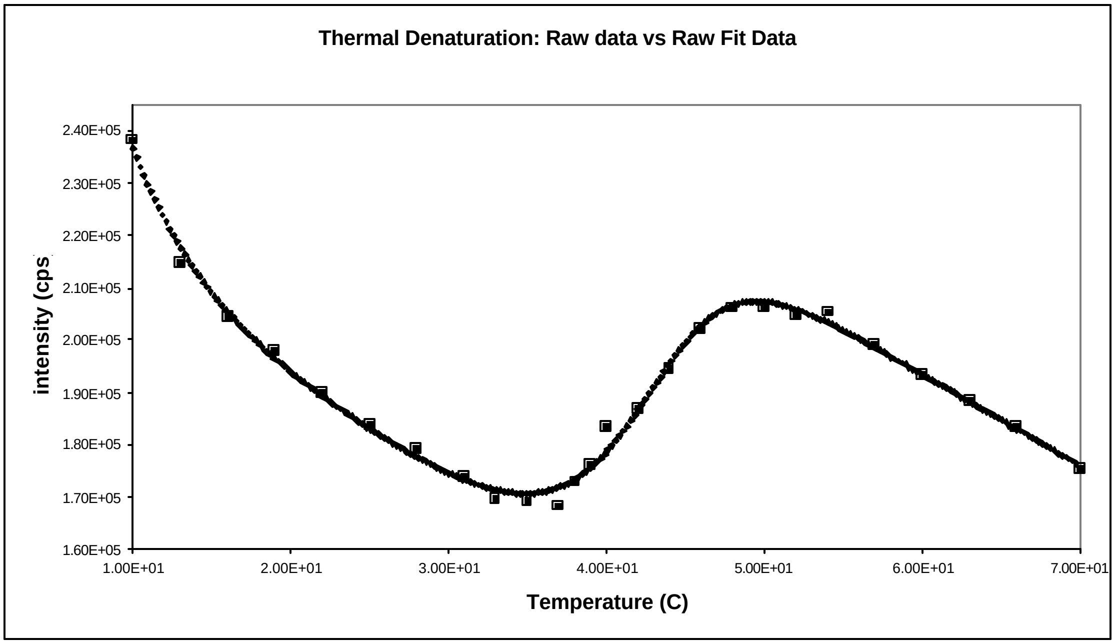

Graph 11 The above graph shows how aconitase reaches its most stable state at 37ºC, and then proceeds to unfold, as indicated by the subsequent increase in fluorescence intensity. Raw data is plotted as (¦).

In order to gain better visualization of the folded and unfolded states, the data was adjusted to show fraction of unfolding versus the folded state. The Fapp fittings shown below illustrate how the fluorescent intensity seen at the folded state is considered to be a low fraction of the final, unfolded fluorescent signal.

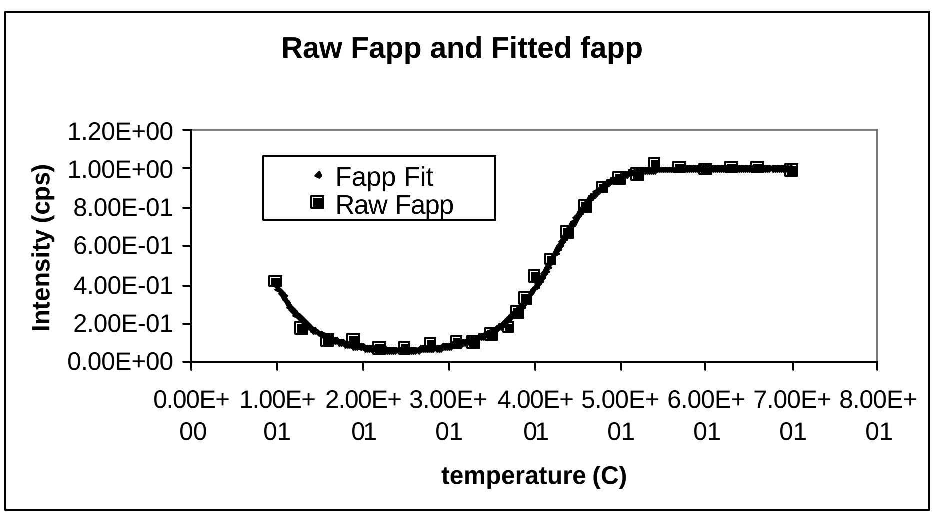

Graph 12 The above data has been normalized and the raw data is plotted as (¦) on top of the Fitted Fapp data.

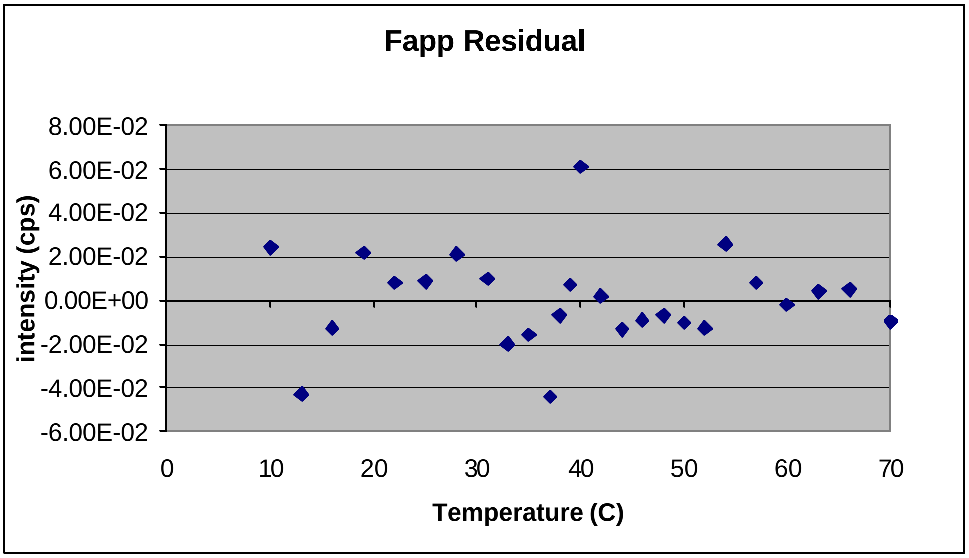

Graph 13 The above residuals for the data fit show that the standard deviation for the fit was random.

Tm (Celsius) = 41.7
dH(Tm) (kcal/mol) = 61.1
Cp(U)-Cp(N) (kcal/mol-deg = 3.57

Chart 1 The above chart shows the calculated values for melting temperature(Tm), changes in enthalpy (?H), and changes in heat capacity (?C_p).

The calculated change in enthalpy is 61.11 (kcal/mol), and this value is a numerical representation of the amount of energy required to denature the protein. Energy had to be added to the protein in order to denature it from its most stable, folded state.

Enthalpy is one of the main factors that determine a value for Gibb's free energy, and enthalpy also gives a sense of stability. By definition, enthalpy is the heat absorbed by a system at constant pressure (Haynie, 32). Stated more simply, enthalpy is the amount of energy a particular system has that can be given up to surrounding systems. A spontaneous reaction will have a negative enthalpy value, and coupled with higher magnitudes, a negative enthalpy reflects a release of energy from the system to surroundings.

When heat, a manifestation of work and a fundamental expression of energy, is released, less energy is needed to hold a system together. By requiring less internal energy, a system is brought to a more stable, favorable state.

The calculated ?Cp is 3.57 and the positive value means the unfolded state has a higher heat capacity than the folded, native state. This is an expected outcome because water molecules, which arrange themselves around the exposed residues of the unfolded state, impose greater order and energy to the unfolded state.

Calculation of a Gibb's Free Energy

Gibb's Free energy is not an actual value that represents a quantified physical characteristic. The Gibb's free energy gives an indication of stability because it accounts for two fundamental properties in thermodynamics, entropy (S) and enthalpy (H).

Entropy is a term, that in its most general sense, measures randomness. According the second fundamental law of thermodynamics, all processes in the universe spontaneously move to a more favorable, disordered state. A simple example of this principle is the diffusion of perfume throughout a room after being sprayed. In fact, "most scientists consider the Second Law of Thermodynamics the most universal 'governor' of natural activity that has ever been revealed by scientific study" (Haynie, 53).

As proteins unfold, higher states of disorder or entropy ensue. Based on the amount of entropy the folded state lacked, a relative measure of energy can be ascertained from the energy emplo yed to prevent spontaneous unfolding.

Gibb's Free Energy takes both enthalpy and entropy into account because often a process might be favored in terms of entropy but not enthalpy, or vice versa. Eventually, the magnitude

and direction of these two factors yield an overall numerical value indicating the spontaneity or stability of a system.

Gibb's Free Energy also is mathematically related to equilibrium constants as shown below. The thermodynamic stability of the protein, numerically represented by a Gibbs's free energy value, can be determined by using the following relationship

$$\Delta G^\circ = -RT \ln K_{eq}$$

K is the equilibrium constant for the unfolding reaction, R is the gas constant, and T is the temperature in Kelvin degrees

Experimental Conclusions

Though originally meticulously planned, numerous unexpected results forced the experimental method to be modified repeatedly. Original plans called for investigation of the h-IRP/aconitase equilibrium properties, kinetic properties, and possibly an investigation into the effects of oxidants on the aconitase structure and activity. Although these original plans were not all carried out, the natural course of research led to interesting results nonetheless.

The results discussed above, and the theory supporting either the results or the experimental methods can be drawn together and a preliminary model of structural features and equilibrium properties to be presented.

Clearly, highly purified and active aconitase was successfully synthesized repeatedly throughout the research year. Numerous modifications to the preparation were made, and a clear and reliable method of producing aconitase at USNA has been established.

With the addition of urea, fluorescent intensity increased as well. Alignment of linear sequences of porcine aconitase and c-aconitase suggests a coupling of substituted tryptophans

129 and 527 in the *m*-aconitase coding sequence. The fluorescent data supports the model developed using homologue alignment. Experimental controls using the Sigma porcine heart showed a decrease in fluorescence with the additions of denaturant. Since the porcine heart aconitase does not have the coupled tryptophans, experimental observations concur with structural features.

The thermal denaturation curves do not show a red shift in the unfolded state, but the urea denaturation curves do show the red shift. The red shift indicates increased exposures of side chains to the energy absorbing effects of an aqueous solvent. This difference between these two experimental methods indicates a differing mechanism for unfolding of the protein. In fact, the different red shifts also possibly indicate different end state products of the two unfolded states.

Furthermore, the thermal data shows a simple, cooperative mechanism. The urea denaturation consistently demonstrated a multi-state, complex unfolding mechanism. At least three equilibrium states appear to have been observed.

The denaturing of c-aconitase can be correlated with loss of enzymatic activity. At about 2.4 M [urea], both an equilibrium state of denaturing occurs as well as a loss of activity. These corresponding events indicate loss of the Fe-S core has occurred or perhaps the loss of just one iron from the cluster. Literature indicates the cluster removal process is slow and controlled (cite), though the loss of one iron from the cluster will cease enzymatic activity. The loss of activity might also be attributed to a change in the position of domain IV. Initial increases in activity can be related to increased access to the active site by the substrate. However, domain IV is required for stabilization of the enzyme and substrate; and, if the domain is opened too much (Kaldy et al,1999), stabilizing ability might be lost as well.

Additions of EDTA to samples, and subsequent chemical denaturation, demonstrate the iron-sulfur cluster confers little stabilizing affects to the protein scaffolding. Also, the iron (II) does not make a significant difference in the unfolding of the protein.

Novel conclusions reached in the characterization study include the observation of fluorescence increases upon chemical denaturation. This unusual, unexpected result led to a development of a preliminary model of coupled tryptophan residues quenching each other's fluorescing abilities.

Also, the study clearly determined the Fe cluster is not needed for the stabilization of the aconitase. This is consistent with the bifunctional nature of the h-IRP1 and aconitase because the protein must be able to conduct its transcriptional regulation role once it loses its structure.

IV. Discussion

A Question of Bifunctionality

The discovery of c-aconitase began first with the discovery of mitochondrial aconitase. In 1937, Carl Martius "demonstrated that the dehydrogenation of citrate to α-ketoglutarate proceeded in two steps…catalyzed by what was later called aconitase" (Beinert, 93). In fact, early scientific research indicated the presence of both mitochondrial and cytoplasmic aconitase in tissue extracts.

As researchers' efforts became more focused, a clearer picture emerged as to how these two enzymes are related. The two enzymes are distinctly different, and in fact different chromosomes code for each enzyme (Beinert, 1993).

Within the citric acid cycle, the role of mitochondrial aconitase is clear and defined. The enzyme catalyzes an isomerization of citrate into isocitrate, effectively changing the four-carbon

molecule from a tertiary alcohol to a secondary alcohol, which enables further oxidation and subsequent production of energy-producing NADH/NADPH. The metabolic step itself is not particularly useful in terms of oxidation or energy production. Rather, the step is important because it allows the entire cycle to function efficiently.

Also, the production of isocitrate is not a particularly favorable step, even with the catalyzing enzyme. In fact, the equilibrium mixture at 7.4 pH and 25°C contains less than 10% isocitrate (Nelson & Cox, 574). The reaction proceeds due to rapid consumption of the isocitrate (removal of products), and the lowering of the steady state concentration forces the reaction in the forward direction.

Obviously, the function of the mitochondrial aconitase is well understood, as is its structure. Containing 747 amino acids residues, three cysteine residues actually function in the stabilization of the substrate to the cluster active site. Also, mitochondrial aconitase does not have IRE-binding function (Kaldy et al, 1999).

In contrast, the cytosolic form of aconitase differs greatly in function. All aspects of the citric acid cycle occur within the mitochondrial membrane, isolated from the surrounding cytosolic infrastructure. The location of c-aconitase as an enzyme limits its applicability as a citric acid catalyst.

Though the c-aconitase is able to catalyze the same reaction as its mitochondrial homologue, it cannot get into the mitochondria. Though bifunctional in theoretical terms, the enzymatic purpose of c-aconitase remains unsolved.

The General Scheme of Iron Regulation

After the intake of iron, generally through dietary means, iron must be transferred either to the point of incorporation or to a structure designed for the storage of iron. Several proteins are involved in this intricate scheme to maintain iron homeostasis, and the aconitase/h-IRP1 plays a central role in the regulation.

If consumed iron were not bound, and instead allowed to roam throughout the body in its free forms, a cascade of toxic effects would ensue. Unbound iron can catalyze the formation of free radicals (Fenton,10), and these free radicals can cause significant damage to both cellular structure and genetic information. Ultimately, the effects of free radicals and the resultant genetic damage often result in the production of cancerous cells.

The alternate form and function of aconitase, the IRP1, is better understood and more logical. The IRP-1 is the central regulatory factor involved in the post-transcriptional control of the expression of ferritin, erythroid 5-aminolevulinate synthase and transferring receptor (Gray et al, 1993).

The fourth domain is involved with the IRP binding to IRE. Arginines 728 and 732 contact the IRE bulge, and amino acid region 685-689 is necessary for IRE loop recognition (Kaldy et al, 1999).

Ferritin is the chief protein responsible for iron storage. Ferritin is located within numerous mammalian organs including the liver and bone marrow. The ferritin structure is composed of 24 peptide subunits, and the entire structure is capable of holding up to 4500 Fe(III) atoms within the 80 Å core (Fenton, 10-12). The ferritin allows the body to store scarce, but vital iron and also allows for quick mobilization of iron in the case of changing homeostatic conditions.

Once the need for iron arises within the body, a clever scheme for the transport of toxic, insoluble iron is needed. In higher animals, nature's answer to this pressing dilemma comes in the form of transferrin.

Transferrin is a monomeric glycoprotein that binds to Fe(III) tightly, but reversibly. Though the iron is bound deeply within the clefts of two protein domains, flexibility of the two domains might perhaps serve as the unloading mechanism for the iron species.

The final protein post-transcriptionally controlled by the influence of h-IRP1 is erythroid translational 5-aminolevulinate (eALAS). The eALAS protein is not exactly involved with iron regulation, but plays a small, elegant and crucial role in the biosynthesis of heme. Heme is a large organic molecule that binds a single iron atom in its center. This iron atom then binds to a single oxygen molecule, and the oxygen molecule is transported to every area of the body.

Although 85% of heme (Koolman & Röhm, 178) occurs in the bone marrow, a small amount is created within the liver. The heme molecule itself binds iron, and is subsequently incorporated into both oxygen transporting hemoglobin and myoglobin.

The above proteins show the complex control system needed to regulate iron, and the need for iron is clear whether it involves oxygen transport or energy production. The h-IRP element influences mRNA segments of IRE (iron responsive elements) in two ways. If the iron levels of the body are low, and the aconitase has lost its iron sulfur cluster and assumed the IRP form, the IRP is capable of influencing the mRNA.

With lowered iron levels, suppression of ferritin must occur because excessive iron storage is detrimental to the restoration of normal iron levels. The IRP-1 binds to the section of the IRE that actually signals the initiation of ferritin production. When the IRE is bound by a ribosome, and amino acid linkage begins, the protein production will be inhibited by the

blockage of the initiation site (Gray et al, 1993) Likewise, the need for transferrin sharply increases. When the IRP binds to transferrin mRNAs, it confers structural stabilities and prevents the degradation of the RNA by protecting cleavage sites by endoribonucleases (Kaldy et al, 1999). The additional life afforded to the transferrin RNA allows for increased production and transport.

Indications of c-aconitase Function

As research grapples with the implications of the existence of bifunctional proteins, a more fundamental problem exists with the investigation of cytoplasmic aconitase. The physiological role of cytoplasmic aconitase remains unsolved, as does the structure. In fact, only the sequence based on genetic code from the human genome project remains solved. Throughout the year, assumptions were made relating both structure and function of cytoplasmic aconitase to its homologue mitochondrial aconitase (porcine).

Extensive studies involving sequence alignment have been performed, and with confidence researchers have used porcine aconitase as a starting point for structure probes (Gegout et al, 1999) and function assumptions (Kaldy et al, 1999). Advances have been achieved in understanding h-IRP but the c-aconitase continues to elude understanding. In attempting to characterize aconitase throughout the course of the Trident project, significant efforts went into possibly gaining insight into aconitase's physiological role.

Cytoplasmic aconitase does not participate in the Krebs Cycle. Even if the c-aconitase could maintain its sister function, there are no metabolic pathways set up in the cytoplasm.

As stated earlier, production of isocitrate is not very favorable at homeostatic conditions, and the 10% produced is only encouraged by rapid consumption. There is no indication of

isocitrate consumption; therefore, enzymatic activity by the c-aconitase cannot be maintained in the forward direction.

C-aconitase is found in high proliferation within liver cells. Interestingly enough, 15% of all heme molecules are synthesized within the liver, and the eALAS discussed earlier plays a key enzymatic role in the creation of the hepatic heme. The h-IRP, once activated, helps regulate post-transcriptional control of eALAS.

C-aconitase is not a redox protein, like many of its iron-sulfur family members, and its only known role as an enzyme is to confer stabilization to a reaction intermediate.

The extra 135 amino acid sequences in the c-aconitase protein scaffolding in fact allow IRE binding. The m-aconitase lacks the extra loops and displays no IRE binding activity (Kaldy et al, 1999). The m-aconitase and c-aconitase come from different coding chromosomes (Beinert et al, 1993), and with only 27% identity of base sequences, there is little evidence supporting an evolutionary relationship.

The function of aconitases has been highly conserved by nature. Species ranging from *E. coli* to humans have aconitase proteins. The base sequences of three completely solved genomes include human, *Drosophila melangaster* (fruit fly), and *E. coli* (bacterium). Base pair sequence alignment performed on the aconitases of these three species afforded startlingly high conservation of identity and supports theories of c-aconitase being a highly preserved cellular mechanism or even an endosymbiotic relationship.

Organism	Identity
Fruit Fly-Human	67.0% identity
Human-E.Coli	51.6% identity

E.Coli-Fruit Fly	51.6% identity

V. Conclusion

In this characterization study, an increased understanding of features distinguishing human cytoplasmic aconitase was sought by using numerous analytical methods.

The project succeeded by gaining insight into structural features, unfolding processes, and equilibrium properties that characterize the bifunctional protein.

Though the function of cytoplasmic aconitase remains undetermined, the characterization study supports the complexity and versatility of this enzyme. Also, both the functional and genetic relationship between mitochondrial and cytoplasmic aconitase appear diminished at the conclusion of this project.

Future areas of interest concerning this bifunctional enzyme include additional spectroscopic studies, including EPR, and focusing more closely on the thermal transition of 37-40°C where the data fit appeared to deviate.

Further insight into the proposed tryptophan coupling present in the cytoplasmic aconitase could be verified using site-directed mutagenesis and x-ray crystallography.

Much work remains in gaining a more developed understanding of not only the structure of the cytoplasmic aconitase/h-IRP1, but also of the cytoplasmic aconitase function. However, increased understanding will lead to a more complete picture of both iron regulation and cellular resistance to damaging oxidants.

References

1. Atkins, P. 1998. "Sixth Edition: Physical Chemistry." W.H. Freeman and Company. New York.
2. Beinert, H., Kennedy, M.C. 1993. Aconitase, a two-faced protein: enzyme and iron regulatory factor. *FASEB Journal*. 7:1442-1449.
3. Drapier,J.-C., Hibbs, J.B.,Jr. (1986) Murine cytotoxic activated macrophages inhibit aconitase in tumor cells. Inhibition involves the iron-sulfur prosthetic group and is reversible. *J. Clin. Invest.* 78, 790-797.
4. Ebsworth, E.A.V., Rankin, David W.H., Cradock, Stephen. 1991. "Structural Methods in Inorganic Chemistry." CRC Press, Boca Raton.
5. Fan, Y., Ju, M., Tsou, C. 1996. Activation of chicken hydrofolate reductase by urea and guanidine hydrochloride is accompanied by conformational change at the active site. *Biochem. J*, 315, 97-102.
6. Fenton,D. (1995) "Biocoordination Chemistry." Oxford Science Publications. New York.
7. Finn, B., Chen, X., Jennings, P., Saalau-Bethell, S., Matthews, C.R. (1992) "Protein Engineering: A Practical Approach." Principles of protein stability. Part 1-reversible unfolding of proteins: kinetic and thermodynamic analysis. Oxford University Press. New York.
8. Gegout, V., Schlegl, J., Schläger, B., Hentze, M., Reinbolt, J., Ehresmann, B., Ehresmann, C., Romby, P. 1999. Ligand-induced Structural Alterations in Human Iron Regulatory Protein-1 Revealed by Protein Footprinting. *The Journal of Biological Chemistry*, 274, 15052-15058.
9. Gray, N.K., Quick, S., Goossen, B., Constable, A., Hirling, H., Kuhn, L., Hentze, M. 1993. Recombinant iron-regulatory factor functions as a iron-responsive-element-binding protein, a translational repressor and an aconitase. *Eur. J. Biochem*, 218, 657-667.
10. Haynie, D. 2001. "Biological Thermodynamics." Cambridge University Press. Cambridge.
11. http://chemistry.gsu.edu/glactone/PDB/Proteins/Krebs/6acn.html
12. http://lc.chem.ecu.edu/class/mathis/225l/FL.htm
13. http://wine1.sb.fsu.edu/krebs/krebs.htm
14. http://www.awl.com/mathews/ch14/frames.htm
15. http://www.pps99-1.cryst.bbk.ac.uk/projects/gmocz/fluor.htm
16. Kaldy, P., Menotti, E., Moret, R., Kuhn, L. 1999. Identification of RNA-binding surfaces in iron regulatory protein-1. *The EMBO Journal*, 18, 6073-6083.
17. Koolman, J., Röhm, K. 1996. "Color Atlas of Biochemistry." Theime Stuttgart. New York.

    Kraulis, PJ (1991) J. *Applied Crystallography 24*:
18. Nelson, D., Cox, M. 2000. "Third Edition: Lehninger Principles of Biochemistry." Worth Publishers. New York.

19. Paraskeva, E., Hentze, M. 1996. Iron-Sulphur clusters as genetic regulatory switches: the bifuntional iron regulatory protein-1. *FEBS Letters*, 389, 40-43.
20. Protein structures prepared using Molscript.
21. Protein X-ray structure modified using Swiss PDB Viewer 3.7. Guex, N and Peitsch, MC (1997) *Electrophoresis 18*: 2714-2723. URL: www.expasy.ch/spdbv/
22. Reproduced with permission of V.F. Smith, Chemistry Department, USNA. 2001.
23. Rose, I., O'Connell, E. (1967) *J. Biol. Chem*. 242, 1870-1879.
24. Sequence alignment performed using Genestream. Person, WR, Wood, T, Zhang, A and Miller, W. (1997) *Genomics 46*:24-36.
25. www.ncbi.n/m.nih.gov

Appendix A. Data Analysis

1. Thermal Data fitting was performed using a non-linear least squares data fitting program . The UNIX based Savuka version 5.1 was written by Lambright and Bilsel. Access to the online software was made possible by the University of Massachusetss Medical School, C. Robert Matthews Laboratory.

2. RASMOL Molecular Graphic Windows Version 2.6 was used to perform three-dimensional protein viewing.

3. All spreadsheet analysis was performed using Microsoft 2000 ® version (9.0.2720)

4. All alignment studies were performed using the online services DIALIGN version 2.1 and ALIGN. These sites are available at http://us.expasy.org/tools/#align.

5. Protein structures prepared using Molscript.
   Kraulis, PJ (1991) J. *Applied Crystallography 24*: 946-950.

6. Protein X-ray structure modified using Swiss PDB Viewer 3.7. Guex, N and Peitsch MC (1997) *Electrophoresis 18*: 2714-2723. URL: www.expasy.ch/spdbv/

7. Sequence alignment performed using Genestream.
   Person, WR, Wood, T, Zhang, A and Miller, W. (1997)
   Genomics 46:24-36.

8. Illustrations were modified using Corel Draw, version 9.337 © 1988-1999 Corel Corporation.

9. PDC files were obtained from www.rcsb.org/index/html

10. PubMed inc. Blast. www.ncbi.n/m.nih.gov

Appendix B- Materials

All reagents were used as received with the following exceptions:

1. Urea solutions were de-ionized, filtered with a 20 µm filter, and buffered with Tris.
2. Sigma porcine mitochondrial aconitase was filtered using a 20 µm filter.
3. All buffers for spectroscopy were filtered with 20 µm filters.

Thank you to Prof. Matthias Hentze, EMBL, Heidelberg, for providing the plasmid for overexpressing human IRP-1 in *E.coli*.

Appendix C. Additional Protocols

Determination of [urea]: an approximate 10 M [urea] was passed through a Bio-Rad resin and then followed with filtration using a 20 µm filter. [Urea] was determined using an Abbè refractometer. Urea solution was then buffered with 50 mM Tris.

Urea denatured sampled were prepared using a spreadsheet produced matrix of reagent volumes. A sample matrix is provided below

Vial #	[Protein]	[urea]	protein volume	9.72 M urea (uL)	buffer (uL)	total volume (uL)
1	.5 uM	0	250	0	250	500
2	.5 uM	0.2	250	10.28	239.72	500
3	.5 uM	0.4	250	20.57	229.43	500
4	.5 uM	0.6	250	30.85	219.15	500
5	.5 uM	0.8	250	41.14	208.86	500
6	.5 uM	1	250	51.42	198.58	500
7	.5 uM	1.2	250	61.71	188.29	500
8	.5 uM	1.4	250	71.99	178.01	500
9	.5 uM	1.6	250	82.28	167.72	500
10	.5 uM	1.8	250	92.56	157.44	500
11	.5 uM	2	250	102.84	147.16	500
12	.5 uM	2.2	250	113.13	136.87	500
13	.5 uM	2.4	250	123.41	126.59	500
14	.5 uM	2.6	250	133.70	116.30	500
15	.5 uM	2.8	250	143.98	106.02	500
16	.5 uM	3	250	154.27	95.73	500
17	.5 uM	3.2	250	164.55	85.45	500
18	.5 uM	3.4	250	174.84	75.16	500
19	.5 uM	3.6	250	185.12	64.88	500
20	.5 uM	3.8	250	195.40	54.60	500
21	.5 uM	4	250	205.69	44.31	500
22	.5 uM	4.2	250	215.97	34.03	500
23	.5 uM	4.4	250	226.26	23.74	500
24	.5 uM	4.6	250	236.54	13.46	500
25	.5 uM	4.8	250	246.83	3.17	500
26	.5 uM	5	250	257.11	-7.11	500
27	.5 uM	5.2	250	267.40	-17.40	500
28	.5 uM	5.4	250	277.68	-27.68	500
29	.5 uM	5.6	250	287.96	-37.96	500
30	.5 uM	5.8	250	298.25	-48.25	500

Appendix D. Instrumentation

1. HP 8452 UV-Vis Diode Spectroscopic Array- used to develop coupled assay activity and citrate properties
2. Amersham Pharmacia AKTA chromatograph- used to purify aconitase through Ni-NTA column chromatography
3. Gilford UV-Vis Spectrometer- used to track all activity of direct assay
4. Spex Fluorolog-3 Fluorometer- used to perform all fluorescence unfolding studies